Inorganic Chemistry

Article

pubs.acs.org/IC

A Structural and Spectroscopic Investigation of Octahedral Platinum Bis(dithiolene)phosphine Complexes: Platinum Dithiolene Internal Redox Chemistry Induced by Phosphine Association

P. Chandrasekaran,*[,†] Angelique F. Greene,[‡] Karen Lillich,[‡] Stephen Capone,[‡] Joel T. Mague,[‡] Serena DeBeer,[§,⊥] and James P. Donahue*[,‡]

[†]Department of Chemistry and Biochemistry, Lamar University, Beaumont, Texas 77710, United States

[‡]Department of Chemistry, Tulane University, 6400 Freret Street, New Orleans, Louisiana 70118, United States

[§]Department of Chemistry and Chemical Biology, Cornell University, Ithaca, New York 14853, United States

[⊥]Max Planck Institute for Chemical Energy Conversion, Stiftstrasse 34−36, D-45470 Mülheim an der Ruhr, Germany

Supporting Information

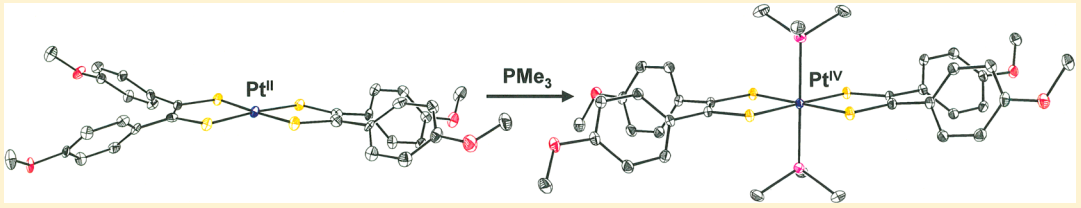

ABSTRACT: The complexes $[Pt(mdt)_2]$ (**4**; mdt = methyldithiolene, $[Me_2C_2S_2]^{n-}$), $[Pt(adt)_2]$ (**5**; adt = *p*-anisyldithiolene, $[(MeO\text{-}p\text{-}C_6H_4)_2C_2S_2]^{n-}$), and $[Pd(adt)_2]$ (**10**) have been prepared in yields of ≥90% via transmetalation reactions with the corresponding $[R_2Sn(S_2C_2R'_2)]$ complexes (R = ^{n}Bu, R′ = Me; R = Me, R′ = $-C_6H_4$-*p*-OMe, **3**). Intraligand C−S and $C-C_{chelate}$ bond lengths (∼1.71 and ∼1.40 Å, respectively) obtained by X-ray crystallography show these compounds to be comprised of radical monoanions $mdt^{\bullet-}$ and $adt^{\bullet-}$. The six-coordinate octahedral adducts $[Pt(adt)_2(dppe)]$ [**6**; dppe = 1,2-bis(diphenylphosphino)ethane], *trans*-$[Pt(adt)_2(PMe_3)_2]$ (**8**), and *trans*-$[Pt(mdt)_2(PMe_3)_2]$ (**9**) have also been prepared, and crystal structures reveal dithiolene ligands that are fully reduced ene-1,2-dithiolates (C−S and $C-C_{chelate}$ = ∼1.77 and 1.35 Å, respectively). Reduction of the dithiolene ligand thus occurs to accommodate the +IV oxidation state typical of octahedral six-coordinate platinum. The cyclic voltammogram of **5** shows two fully reversible reductions at −0.11 and −0.84 V in CH_2Cl_2 (vs Ag/AgCl), attributed to successive ($adt^{\bullet-} + e^- \rightarrow adt^{2-}$) processes, and a reversible oxidation at +1.01 V. The cyclic voltammogram of **9** shows two reversible oxidations at +0.38 and +0.86 V, which are assigned as successive ($adt^{2-} \rightarrow adt^{\bullet-} + e^-$) oxidations. Consistent with their formulation as having fully reduced dithiolene ligands, the UV−vis spectra for **6**, **8**, and **9** show no low-energy absorptions below 700 nm, and the S K-edge XAS spectra of **6** and **8** show dithiolene sulfur that is reduced relative to that in **5**. The introduction of PMe_3 to **10** did not produce the palladium analogue of **8** but rather $[Pd(adt)(PMe_3)_2]$ (**11**). The reaction of $[PdCl_2(PPh_3)_2]$ with $Li_2(mdt)$ produced a mixture of $[Pd(mdt)(PPh_3)_2]$ (**12**, 20%) and $[(Ph_3P)Pd(\mu\text{-}1,2\text{-}mdt\text{-}S,S':S)_2Pd(PPh_3)]$ (**13**, 28%), with the latter having C_2 symmetry with a Pd_2S_2 core structure folded along the S···S axis.

INTRODUCTION

Metallodithiolene complexes, both homoleptic and heteroleptic, have enjoyed continuous scrutiny over the several decades since their initial syntheses and property investigations were disclosed. Much of this activity has been motivated by the promise of applications as catalysts[1] or advanced materials.[2−7] Among heteroleptic complexes, two large classes have been developed, one being mono- and bis(dithiolene) complexes of molybdenum and tungsten because of their biological relevance[8] and the second being mono(dithiolene) complexes of the group 10 metals, in large part owing to the photophysical properties of $[Pt(S_2C_2R_2)L_2]$ complexes.[3−5,9−11]

Compounds of the type $[M(S_2C_2R_2)(phosphine)_2]$ (M = Ni, Pd, Pt) were among the first of this latter class to be described.[12] An early communication by Schrauzer and Mayweg also detailed the preparation and isolation of six-coordinate $[M(S_2C_2R_2)_2(PPh_3)_2]$ species (M = Pd, R = Ph; M = Pt, R = Ph or Me),[13] but a subsequent report by Davison and Howe disputed the identity of the species formed under the given conditions, identifying them instead as $[M(S_2C_2R_2)(PR_3)_2]$ complexes.[14] In a reexamination of the compound type, Schrauzer and Mayweg affirmed the preparation and isolation of blue $[Pt(S_2C_2Ph_2)_2(PR_3)_2]$ (PR_3 = $^1/_2$dppe, P^{n}Bu$_3$) and brown $[Ni(S_2C_2Ph_2)_2(PR_3)_2]$ (PR_3 = PPh_3, P^{n}Bu$_3$), albeit from room temperature reactions rather than from refluxing conditions as initially described.[15] The nickel compounds were noted as being markedly less stable than the platinum

Received: May 31, 2014
Published: August 12, 2014

   dx.doi.org/10.1021/ic501273b | *Inorg. Chem.* 2014, 53, 9192−9205

Table 1. Summary of Known Platinum Dithiolenebis(phosphine) Complexes

compound	reference
[(mnt)Pt(dppe)] [mnt = maleonitriledithiolate(2−) = $[(NC)_2C_2S_2]^{2-}$); dppe = $Ph_2PCH_2CH_2PPh_2$]	18, 19
[(mnt)Pt(P−P)] [P−P = $Ph_2PCH{=}CHPPh_2$, 1,2-$(Ph_2P)_2C_6H_4$, or $Cy_2PCH_2CH_2PCy_2$]	18
[(mnt)Pt($Ph_2PCH_2PPh_2$)]	20
[(mnt)Pt(PR_2R')$_2$] (R = R′ = Ph;[12,18,21] R = Me, R′ = Ph;[18,22] R = R′ = Et[22])	12, 18, 21, 22
[(mnt)Pt($P(CH_2OH)_3$)$_2$]	23
[(mnt)Pt($P(OR)_3$)$_2$] (R = Et or Ph)	20
[(mnt)Pt(abpcd)] [abpcd = 2-(9-anthracenylidene)-4,5-bis(Ph_2P)-4-cyclopenten-1,3-dione]	24
[(mnt)Pt(fbpcd)] [fbpcd = 2-(ferrocenylidene)-4,5-bis(Ph_2P)-4-cyclopenten-1,3-dione]	25
[$(H_2C_2S_2)$Pt(P^nBu_3)$_2$]	26
[$(H_2C_2S_2)$Pt(PR_2R')$_2$] (R = R′ = Et; R = Me, R′ = Ph)	22
[$(H_2C_2S_2)$Pt(PPh_3)$_2$]	21
[$((CF_3)_2C_2S_2)$Pt(PPh_3)$_2$]	12
[$((MeO_2C)_2C_2S_2)$Pt(PPh_3)$_2$]	27
[$((RO_2C)_2C_2E_2)$Pt(dppe)] (R = Me or Et; E = S or Se)	28
[$((MeO_2C)_2C_2S_2)$Pt($P(OMe)_3$)$_2$]	29
[$(Ph_2C_2S_2)$Pt(P−P)] (P−P = dppe or $2PPh_3$)	16
[$(($t$Bu-$p$-$C_6H_4)_2C_2S_2)$Pt($PPh_3$)$_2$]	30
[((ArH)C_2S_2)Pt(dppe)] (Ar = 2-pyridyl,[31] 3-pyridyl,[31] 2-quinoxalinyl,[31,32] 2-pyrazinyl[31])	31, 32
[(O=$CS_2C_2S_2$)Pt(P−P)] (P−P = dppe or $2PPh_3$)	21, 33, 34
[(S=$CS_2C_2S_2$)Pt(PPh_3)$_2$] [S=$CS_2C_2S_2$ = 1,3-dithiole-2-thione-4,5-dithiolate(2−)]	21, 33, 35
[(S=$CS_2C_2S_2$)Pt(PEt_3)$_2$]	36
[(S=$CS_2C_2S_2$)Pt($Ph_2PCH_2CH_2PPh_2$)]	35
[(S=$CS_2C_2S_2$)Pt(3,4-Me_2-3′,4′-$(Ph_2P)_2$ttf] (ttf = tetrathiafulvalene)	37
[(S=$CS_2C_2S_2$)Pt(dppf)] [dppf = 1,1′-bis(diphenylphosphino) ferrocene = $(C_5H_4(Ph_2P))_2Fe$]	38
[(S=$CS_2C_2S_2$)Pt(DPCB)][a]	39
[(S=$CS_2C_2S_2$)Pt(DPCB-phen)][b]	39
[(dddt)Pt(PPh_3)$_2$] [dddt = 5,6-dihydro-1,4-dithiin-2,3-dithiolate (2−)]	21
[(dddt)Pt(dppe)]	40
[(dddt)Pt(3,4-Me_2-3′,4′-$(Ph_2P)_2$ttf)]	40
[(dddt)Pt(dppf)]	38
[(mtdt)Pt(dppf)] [mtdt = 1,2-bis(methylthio)ethylene-1,2-dithiolate(2−)]	38
[(phdt)Pt(dppf)] [phdt = 6-hydro-5-phenyl-1,4-dithiin-2,3-dithiolate(2−)]	38
[(dphdt)Pt(dppf)] [dphdt = 5,6-diphenyl-1,4-dithiin-2,3-dithiolate(2−)]	38
[(bdt)Pt(PPh_3)$_2$] [bdt = benzene-1,2-dithiolate(2−)]	41
[(bdt)Pt(dppf)]	42
[(bdt)Pt(3,4-Me_2-3′,4′-$(Ph_2P)_2$ttf)]	40
[(bdt)Pt(DPCB)][a]	39
[(bdt)Pt(DPCB-phen)][b]	39
[(bdt)Pt(PPh_2(C≡CPh))$_2$]	43
[(bdt)Pt(μ-$Ph_2PC{\equiv}CPPh_2$)$_2$Pt(bdt)]	44
[(2,6-Cl_2-bdt)Pt(dppf)]	42
[(2,6-Cl_2-bdt)Pt(μ-$Ph_2PC{\equiv}CPPh_2$)$_2$Pt(2,6-Cl_2-bdt)]	44
[{4-[(4-methylphenyl)azo]-1,2-bdt}Pt(dppe)]	45, 46
[(tdt)Pt(dppf)] [tdt = toluene-3,4-dithiolate(2−)]	42, 47
[(tdt)Pt(pbpcd)] [pbpcd = 2-(pyrene-1-ylidene)-4,5-bis(Ph_2P)-4-cyclopenten-1,3-dione]	48
[(tdt)Pt(bpcd)] [bpcd = 4,5-bis(Ph_2P)-4-cyclopenten-1,3-dione]	48
[(tdt)Pt(μ-$Ph_2PC{\equiv}CPPh_2$)$_2$Pt(tdt)]	44
[(qdt)Pt(PR_2R')$_2$] [qdt = quinoxaline-2,3-dithiolate(2−); R = R′ = Et; R = Me, R′ = Ph]	22

[a]DPCB = 1,2-diphenyl-3,4-bis[(2,4,6-tri-*tert*-butylphenyl)-phosphinidene]cyclobutene. [b]DPCB-phen = phenanthrene-1,2-diylidene-3,4-bis[(2,4,6-tri-*tert*-butylphenyl)phosphinidene]cyclobutene.

analogues. Since that time, apart from a note of cyclic voltammetry data for $[Pt(S_2C_2Ph_2)_2(dppe)]$[16] [dppe = 1,2-bis(diphenylphosphino)ethane] and a later report describing its use as a dithiolene transfer agent,[17] no published work of which we are aware has revisited these compounds and addressed the correctness of their formulation by Schrauzer and Mayweg or sought to characterize them more thoroughly.

As part of a program of research aimed at a "bottom-up" approach to the synthesis of complex metallodithiolene materials, we have made observations that corroborate Mayweg and Schrauzer's report of isolable $[M(S_2C_2R_2)_2(PR_3)_2]$ complexes,[15] at least with platinum. Considering the fairly extensive corpus of $[M(S_2C_2R_2)(PR_3)_2]$ (M = Ni, Pd, Pt) complexes that has been developed since Mayweg and Schrauzer's work (Table 1), it is surprising that Schrauzer's six-coordinate $[Pt(S_2C_2R_2)_2(PR_3)_2]$ compounds have not been reexamined using modern physical methods of analysis and characterization. Herein we describe the properties and characterization of $[Pt(S_2C_2R_2)_2(PR'_3)_2]$ [R = *p*-anisyl or Me, R′ = Me; R = *p*-anisyl, $(PR'_3)_2$ = 1,2-bis(diphenylphosphino)-ethane] structurally by X-ray crystallography and spectroscopically by S K-edge X-ray absorption spectroscopy (XAS). The latter technique is decisive in showing how the redox noninnocent nature of the dithiolene ligand enables internal redox change between metal and the dithiolene ligand such that the Pt^{IV} oxidation state is created and the expanded coordination sphere is accommodated. Related complexes of palladium are also reported here.

EXPERIMENTAL SECTION

General Considerations. Air- and moisture-sensitive compounds were prepared and handled under a N_2 atmosphere using a drybox or standard Schlenk-line techniques. Published procedures were employed in the syntheses of $[(Me_2C_2S_2)Sn(^nBu)_2]$[49] and $Me_2C_2S_2C{=}O$.[50] All other reagents were purchased from commercial sources and used as received [K metal, CS_2, desoxyanisoin, *N*-bromosuccinimide (NBS), 2,2′-azobis(2-methylpropionitrile) (AIBN), H_2SO_4, ^{n}BuLi (1.6 M in hexanes), Me_2SnCl_2, $PtCl_2$, $PdCl_2$, *cis*-$[Pd(PPh_3)_2Cl_2]$, I_2, PMe_3 (1.0 M in toluene), 10% LiOMe in MeOH, and 1,2-bis(diphenylphosphino)ethane (dppe)]. Solvents were dried with a system of drying columns from the Glass Contour Company [CH_2Cl_2, tetrahydrofuran (THF), and Et_2O], were freshly distilled according to standard procedures (MeOH, MeCN, and 1,2-dichloroethane),[51] or were used as received (CCl_4 and ^{i}PrOH). Silica columns were run in the open air using 60−230 μm silica (Dynamic Adsorbents). The compounds reported and their supporting ligands are hereafter referred to by the numerical designations and abbreviations given in Chart 1.

Instrumentation. All NMR spectra were recorded at 25 °C with a Varian Unity Inova spectrometer operating at 400, 100.5, and 161.8 MHz for ^{1}H, ^{13}C, and ^{31}P nuclei, respectively. Spectra were referenced to the protonated solvent residual for ^{1}H and ^{13}C NMR, whereas 85% H_3PO_4 was used as an external standard for ^{31}P NMR. IR spectra were taken as pressed KBr pellets with a Thermo Nicolet Nexus 670 Fourier transform infrared instrument in absorption mode, while UV−vis spectra were obtained at ambient temperature with a Hewlett-Packard

dx.doi.org/10.1021/ic501273b | Inorg. Chem. 2014, 53, 9192−9205

Chart 1. Numerical Identification System for Compounds

Dithiocarbonic acid *rac*-[1,2-bis(4-methoxyphenyl)-2-oxoethyl] ester *O*-isopropyl ester	**1**
[(MeO-*p*-C_6H_4)$_2$$C_2S_2$C=O]	**2**
[(adt)$SnMe_2$][a]	**3**
[Pt(mdt)$_2$][b]	**4**
[Pt(adt)$_2$][a]	**5**
[Pt(adt)$_2$(dppe)][a,c]	**6**
[Pt(adt)(dppe)][a,c]	**7**
trans-[Pt(adt)$_2$(PMe_3)$_2$][a]	**8**
trans-[Pt(mdt)$_2$(PMe_3)$_2$][b]	**9**
[Pd(adt)$_2$][a]	**10**
[Pd(adt)(PMe_3)$_2$][a]	**11**
[Pd(mdt)(PPh_3)$_2$][b]	**12**
[Pd$_2$(μ-mdt)$_2$(PPh_3)$_2$][b]	**13**

Footnote a: adt = *cis*-1,2-di-*p*-anisyldithiolene, [(MeO-*p*-C_6H_4)$_2$$C_2S_2$]$^{n-}$. Footnote b: mdt = *cis*-1,2-dimethyldithiolene, [$Me_2C_2S_2$]$^{n-}$. Footnote c: dppe = 1,2-bis(diphenylphosphino)ethane.

8452A diode-array spectrophotometer. Electrospray ionization mass spectrometry (ESI-MS) spectra were obtained with either a Bruker Daltonics or a PESciex Qstar instrument. Electrochemical measurements were made with a CHI620C electroanalyzer workstation using a Ag/AgCl reference electrode (or silver wire electrode for [Pt(adt)$_2$(dppe)]), a platinum disk working electrode, a platinum wire auxiliary electrode, and [^{n}Bu$_4$N][PF_6] as the supporting electrolyte. Under these conditions, the [Cp_2Fe]$^+$/Cp_2Fe couple consistently occurred at +440 mV. Elemental analyses were performed by Midwest Microlab, LLC, of Indianapolis, IN. Descriptions of the instrumentation and procedures employed in X-ray diffraction data collection and processing, and for the structure solutions and refinements, are deferred to the Supporting Information (SI), as are figures showing the complete atom labeling for all compounds (Figures S1−S16 in the SI). Unit cell data and refinement statistics for all structures reported are presented in Table 2.

XAS. XAS spectra were measured at the Stanford Synchrotron Radiation Lightsource (SSRL). S K-edge data were obtained using the 20-pole wiggler beamline 4-3. Detailed S K-edge data collection and normalization procedures were followed as previously described.[52] Pt L-edge XAS were measured on the 20-pole wiggler beamline 7-3. Samples for Pt L-edge XAS were prepared by dilution in boron nitride (BN), pressed into a pellet, and sealed between 38 μm Kapton tape windows in a 0.5 mm aluminum spacer. Data were measured in transmittance mode, and samples were maintained at 10 K using an Oxford Instruments CF1208 continuous-flow liquid-helium cryostat. Internal energy calibrations were performed by simultaneous measurement of the Pt reference foil placed between the second and third ionization chambers with inflection points assigned as 13879.9 eV for the L_1-edge. Data were averaged using *EXAFSPAK*[53] and normalized by subtracting the spline and normalizing the postedge to 1.0. The S K pre-edge features were modeled with line shapes having fixed mixing ratios (1:1) of Lorentzian and Gaussian functions (pseudo-Voigt) using the program *EDG_FIT*.[53]

Syntheses. *Potassium O-Isopropylxanthate.* A 1000 mL Schlenk flask was charged with a large stir bar and 2-propanol (700 mL, 550 g, 9.15 mol), capped with a rubber septum, and affixed to a Schlenk line via its side stopcock. While being vigorously stirred, 2-propanol was thoroughly sparged for 15 min with dry N_2 delivered from the inert gas manifold of a Schlenk line through a long syringe needle penetrating the septum and vented through a second, smaller syringe needle. After thorough degassing, 2-propanol was maintained under a positive N_2 pressure applied through the side stopcock of the flask and was cooled to 0 °C with an ice bath. ***Note!*** *It is important for safety reasons that* ^{i}*PrOH be completely oxygen free.* H_2*(g) evolved by the reaction of* K^0 *with* ^{i}*PrOH is very flammable and should be vented through the pressure release system of the Schlenk line into the back of a well-ventilated fume hood.* Pieces of freshly cut K metal (60.1 g total, 1.53 mol) washed with several portions of hexanes were added over a period of 4 h to 2-propanol under a N_2 flow. Vigorous evolution of H_2 gas and moderate warming of the flask ensued. During this time, the 2-propanol solution thickened visibly. The mixture was gradually warmed to ambient temperature, and stirring was continued for approximately 8 h until all K metal had been consumed. With a flow of N_2 outward, the central neck of the Schlenk flask was replaced with a 125 mL pressure equalizing addition funnel fitted with a Teflon stopcock. The $K^+Pr^iO^-$/Pr^iOH mixture was cooled again to 0 °C in an ice bath. Carbon disulfide (100 mL, 126 g, 1.65 mol) was added to the addition funnel and admitted dropwise to the isopropoxide solution over the course of 2 h. A fine, pale-yellow precipitate formed immediately. The reaction vessel was maintained in the ice bath because of the moderate exothermicity of the reaction. Before the addition was complete, the mixture thickened significantly. After the complete addition of CS_2, the addition funnel was replaced with an overhead mechanical stirrer fitted to a Teflon paddle with a suitable adaptor supporting the glass shaft of the stirrer in the neck of the flask. The reaction mixture was warmed to room temperature and subjected to vigorous stirring for 1 h. The thick, pasty potassium *O*-isopropylxanthate was then collected on a large Buchner funnel in the open air and washed with diethyl ether (5 × 100 mL). The slightly moist filter cake was transferred to a clean 1000 mL Schlenk flask, dried at 0.1 Torr at room temperature for 24 h, and obtained as a loose, pale-yellow solid in a yield of 95% (254 g, 1.46 mol). Potassium *O*-isopropylxanthate thus obtained is stable to air, moisture, and light and is of sufficient purity for the following step.

[(MeO-p-C_6H_4*)C(=O)CH(SC(=S)O*^{i}*Pr)(*C_6H_4*-p-OMe)] (**1**).* A 500 mL Schlenk flask with a stir bar was charged with desoxyanisoin (15.0 g, 58.5 mmol), NBS (10.42 g, 58.54 mmol), and AIBN (0.020 g) under an atmosphere of N_2. Following the addition of CCl_4 (200 mL), a reflux condenser was fit to the Schlenk flask and the mixture was heated to 70 °C for 6 h under N_2. After this reaction vessel cooled to room temperature, solid potassium *O*-isopropylxanthate (10.2 g, 58.5 mmol) was added to the reaction mixture in a single portion. With vigorous stirring, the resulting pale-yellow reaction mixture was heated to reflux for 4 h. The mixture was permitted to cool and then was poured over ice water and extracted with portions of CH_2Cl_2 (3 × 150 mL). The combined organic fractions were washed thoroughly with deionized water, dried over $MgSO_4$, and separated from the drying agent by filtration. The filtrate was concentrated under reduced pressure to afford a brown paste. The addition of MeOH to this pasty brown solid residue produced a white solid precipitate, which was collected onto a glass frit by filtration and then dried under vacuum to afford **1**. Yield: 17.73 g, 45.40 mmol, 78%. Mp: 83−85 °C. R_f = 0.52 (3:1 CH_2Cl_2/hexanes). ^{1}H NMR (δ, ppm in $CDCl_3$): 7.99 (d, *J* = 9.2 Hz, 2H, *Ph*), 7.33 (d, 2H, *Ph*), 6.88 (d, *J* = 9.2 Hz, 2H, *Ph*), 6.81 (d, 2H, *Ph*), 6.48 (s, 1H, C*H*), 5.64 (sep, *J* = 6.4 Hz, 1H, C*H*(CH_3)$_2$), 3.82 (s, 3H, −OCH_3), 3.73 (s, 3H, −OCH_3), 1.24 (m, 6H, (CH_3)$_2$CH). ^{13}C NMR (δ, ppm in $CDCl_3$): 212.91 (s, CO), 192.87 (*C*S), 164.34 (s, *Ph*), 160.38 (s, *Ph*), 131.99 (s, *Ph*), 130.95 (s, *Ph*), 129.24 (s, *Ph*), 125.95 (s, *Ph*), 115.30 (s, *Ph*), 114.58 (s, *Ph*), 79.00 (*C*S), 59.98 (CH(CH_3)$_2$), 56.17 (s, −OCH$_3$), 55.94 (s, −OCH$_3$), 21.93 (s, CH(CH_3)$_2$. IR (cm^{-1} in KBr): 2977 (w), 1671 (s), 1597 (s), 1509 (s), 1462 (m), 1242 (s), 1171 (s), 1087 (s), 1039 (s), 864 (w), 782 (m), 597 (m), 530 (m). ESI-MS$^+$: *m*/*z* 391.10 (M + H$^+$). Anal. Calcd for $C_{20}H_{22}S_2O_4$: C, 61.51; H, 5.67. Found: C, 61.82; H, 5.69.

[(MeO-p-C_6H_4*)$_2$*C_2S_2*C=O] (**2**).* A 250 mL three-necked flask equipped with an addition funnel was charged with **1** (17.73 g, 45.4 mmol) and a magnetic stir bar. Over a period of 30 min at 0 °C, 100 mL of 80% aqueous H_2SO_4 was added dropwise directly onto solid **1**. The resulting reaction mixture was stirred well for the ensuing 4 h, during which time it darkened progressively to a brown color. It was then poured over ice and extracted with portions of CH_2Cl_2 (3 × 100 mL). The combined CH_2Cl_2 extracts were washed with saturated aqueous $NaHCO_3$ and then deionized water. This organic solution was then dried over $MgSO_4$, separated from the drying agent by filtration, and reduced to a pasty solid with the use of a rotary evaporator. Methyl alcohol (∼100 mL) was added to this solid residue until a clean product was precipitated. Yield: 12.73 g, 38.52 mmol, 85%. Mp: 138−140 °C. R_f = 0.61 (3:1 CH_2Cl_2/hexanes). ^{1}H NMR (δ, ppm in

dx.doi.org/10.1021/ic501273b | *Inorg. Chem.* 2014, 53, 9192−9205

Table 2. Unit Cell and Refinement Data for Compounds 1−13

	1	2	3	4
formula	$C_{22}H_{22}O_4S_2$	$C_{17}H_{14}O_3S_2$	$C_{18}H_{20}O_2S_2Sn$	$C_8H_{12}PtS_4$
fw	390.50	330.40	451.15	431.51
cryst syst	monoclinic	triclinic	monoclinic	triclinic
space group	$P2_1/c$	$P\bar{1}$	$P2_1/n$	$P\bar{1}$
color, habit	colorless, parallelpiped	colorless, parallelpiped	colorless, parallelpiped	black, prism
a, Å	11.527(1)	5.4968(4)	13.4064(19)	6.9778(14)
b, Å	16.947(2)	11.7792(9)	10.7853(15)	7.1911(14)
c, Å	10.322(1)	12.5653(9)	25.900(4)	7.5203(15)
α, deg	90	113.349(1)	90	62.622(3)
β, deg	102.779(2)	94.108(1)	99.379(2)	62.445(2)
γ, deg	90	94.857(1)	90	88.558(3)
V, Å^3	1966.5(4)	739.33(9)	3694.8(9)	288.52(10)
T, K	100	100	100	100
Z	4	2	8	1
density, g·cm^{-1}	1.319	1.484	1.622	2.483
μ, mm^{-1}	0.292	0.369	1.615	12.833
cryst size, mm	0.10 × 0.11 × 0.17	0.09 × 0.09 × 0.25	0.10 × 0.19 × 0.33	0.05 × 0.05 × 0.11
R1,[a] wR2[b]	0.0710, 0.1492	0.0288, 0.0749	0.0194, 0.0485	0.0160, 0.0390
GOF[c]	1.222	1.065	1.069	1.031

	5·DCE	6	7·DCE	8	9
formula	$C_{34}H_{32}Cl_2O_4PtS_4$	$C_{58}H_{52}O_4P_2PtS_4$	$C_{44}H_{42}Cl_2O_2P_2PtS_2$	$C_{38}H_{46}O_4P_2PtS_4$	$C_{14}H_{30}P_2PtS_4$
fw	898.83	1198.27	994.83	952.02	583.65
cryst syst	triclinic	orthorhombic	monoclinic	monoclinic	orthorhombic
space group	$P\bar{1}$	$Pccn$	$P2_1/n$	$P2_1/n$	$Cmca$
color, habit	orange, plate	blue, plate	yellow, slat	orange, column	orange, plate
a, Å	9.140(6)	17.8597(12)	23.093(4)	8.4203(9)	15.543(3)
b, Å	12.279(8)	18.7052(12)	13.429(2)	13.7295(14)	12.222(2)
c, Å	17.818(12)	16.6577(11)	27.953(5)	33.591(4)	11.3826(18)
α, deg	109.932(9)	90	90	90	90
β, deg	95.950(10)	90	110.592(2)	93.757(1)	90
γ, deg	109.328(8)	90	90	90	90
V, Å^3	1720(2)	5564.8(6)	8115(2)	3875.0(7)	2162.2(6)
T, K	100	100	100	100	195
Z	2	4	8	4	4
density, g·cm^{-1}	1.735	1.430	1.629	1.632	1.793
μ, mm^{-1}	4.513	2.773	3.809	3.958	7.017
cryst size, mm	0.02 × 0.08 × 0.09	0.02 × 0.10 × 0.21	0.10 × 0.16 × 0.28	0.08 × 0.12 × 0.18	0.05 × 0.10 × 0.13
R1,[a] wR2[b]	0.0562, 0.1384	0.0236, 0.0538	0.0262, 0.0520	0.0193. 0.0426	0.0178, 0.0442
GOF[c]	1.012	1.091	1.035	1.046	1.076

	10	11	12	13
formula	$C_{32}H_{28}O_4PdS_4$	$C_{22}H_{32}O_2P_2PdS_2$	$C_{40}H_{36}P_2PdS_2$	$C_{44}H_{42}P_2Pd_2S_4$
fw	711.18	560.94	749.15	973.76
cryst syst	triclinic	monoclinic	monoclinic	triclinic
space group	$P\bar{1}$	$P2_1/c$	Pn	$P\bar{1}$
color, habit	orange, parallelpiped	orange, slab	blue, block	red, block
a, Å	9.792(3)	8.9483(6)	9.0024(4)	9.8658(3)
b, Å	12.201(3)	20.1445(14)	10.9590(4)	10.4704(3)
c, Å	14.106(4)	14.4855(10)	17.4224(7)	21.2026(7)
α, deg	104.443(4)	90	90	85.809(1)
β, deg	104.466(4)	106.924(1)	99.862(10)	83.237(1)
γ, deg	105.890(4)	90	90	68.470(1)
V, Å^3	1475.3(7)	2498.1(3)	1693.5(1)	2022.15(11)
T, K	100	100	100	100
Z	2	4	2	2
density, g·cm^{-1}	1.601	1.491	1.469	1.599
μ, mm^{-1}	0.949	1.054	0.794	1.207
cryst size, mm	0.03 × 0.03 × 0.08	0.11 × 0.16 × 0.23	0.13 × 0.18 × 0.23	0.10 × 0.13 × 0.13
R1,[a] wR2[b]	0.0523, 0.1218	0.0215, 0.0535	0.0169, 0.0446	0.0208, 0.0509
GOF[c]	0.977	1.058	1.131	1.056

dx.doi.org/10.1021/ic501273b | Inorg. Chem. 2014, 53, 9192−9205

Table 2. continued

[a]R1 = $\sum||F_o| - |F_c||/\sum|F_o|$. [b]wR2 = $\{[\sum w(F_o^2 - F_c^2)/\sum w(F_o^2)^2]\}^{1/2}$; $w = 1/[\sigma^2(F_o^2) + (xP)^2]$, where $P = (F_o^2 + 2F_c^2)/3$. [c]GoF = $\{\sum[w(F_o^2 - F_c^2)^2]/(n - p)\}^{1/2}$, where n = number of reflections and p= total number of parameters refined.

$CDCl_3$): 7.11 (d, J = 9.2 Hz, 4H, *Ph*), 6.76 (d, 4H, *Ph*), 3.76 (s, 6H, $-OCH_3$). ^{13}C NMR (δ, ppm in $CDCl_3$): 191.36 (s, *C*O), 160.02 (s, olefinic *C*), 131.14 (s, *Ph*), 127.84 (s, *Ph*), 124.45 (s, *Ph*), 114.53 (s, *Ph*), 55.66 (OCH_3). IR (cm^{-1} in KBr): 1658 (m), 1631 (s), 1600 (m), 1511 (s), 1294 (m), 1248 (vs), 1186 (m), 1027 (m), 832 (s), 584 (w), 518 (w). ESI-MS^+: m/z 331.04 ($M + H^+$). Anal. Calcd for $C_{17}H_{14}S_2O_3$: C, 61.79; H, 4.27. Found: C, 61.68; H, 4.29.

[(adt)SnMe$_2$] ***(3)***. A stirred solution of **2** (4.00 g, 12.1 mmol) in THF (80 mL) under N_2 in a 200 mL Schlenk flask was cooled to 0 °C and treated with ^{n}BuLi in hexanes (1.6 M, 15.13 mL, 24.21 mmol) delivered via syringe. The mixture was stirred for 24 h at ambient temperature, whereupon a solution of Me_2SnCl_2 (2.65 g, 12.10 mmol) in THF (20 mL) was transferred via a cannula at room temperature. This mixture was stirred overnight, quenched by pouring over ice, and then extracted with portions of CH_2Cl_2 (3 × 100 mL). The combined organic fractions were dried over $MgSO_4$. Following removal of $MgSO_4$ and the solvent, the crude product was purified on a silica column eluted with 3:1 CH_2Cl_2/hexanes. Yield: 4.10 g, 8.79 mmol, 73%. Mp: 173−175 °C. R_f = 0.66 (CH_2Cl_2). ^1H NMR (δ, ppm in $CDCl_3$): 7.02 (d, J = 8.8 Hz, 4H, *Ph*), 6.60 (d, J = 9.2 Hz, 4H, *Ph*), 3.69 (s, 6H, $-OCH_3$), 1.01 (s, $J^{119}{}_{Sn-H}$ = 61.6 Hz, $J^{117}{}_{Sn-H}$ = 58.8 Hz, 6H, $Sn(CH_3)_2$). ^{13}C NMR (δ, ppm in $CDCl_3$): 158.53 (s, olefinic *C*), 133.91 (s, *Ph*), 133.41 (s, *Ph*), 130.42 (s, *Ph*), 113.66 (s, *Ph*), 55.63 (s, $-OCH_3$), 3.55 (s, $Sn(CH_3)_2$). ESI-MS^+: m/z 452.99 ($M + H^+$). Anal. Calcd for $C_{18}H_{20}O_2S_2Sn$: C, 47.92; H, 4.47; S, 14.21. Found: C, 48.06; H, 4.49; S, 14.03.

[Pt(mdt)$_2$] ***(4)***. A procedure similar to that implemented for the synthesis of $[Pt(adt)_2]$ (**5**) was followed on a scale employing 0.264 g of $[(mdt)Sn(^nBu)_2]$ (0.989 mmol), 0.100 g of $PtCl_2$ (0.376 mmol), and 0.095 g of I_2 (0.374 mmol). Yield: 0.156 g, 0.362 mmol, 96%. ^1H NMR (δ, ppm in $CDCl_3$): 2.59 (s, 12H, $-CH_3$). ^{13}C NMR (δ, ppm in $CDCl_3$): 177.34 (s), 160.70 (s).

[Pt(adt)$_2$] ***(5)***. A 50 mL Schlenk flask with stir bar was charged with CH_2Cl_2 (30 mL), **3** (0.351 g, 0.778 mmol), and $PtCl_2$ (0.100 g, 0.376 mmol). The resulting reaction mixture was stirred for 12 h at ambient temperature, after which time I_2 (0.095 g, 0.374 mmol) was added in a single portion under a N_2 flow. The dark reaction mixture that resulted was stirred an additional 4 h. The solvent was removed under reduced pressure, and the solid residue was washed with MeOH (2 × 10 mL), followed by Et_2O (3 × 10 mL). The resulting dark solid was dried under vacuum for 24 h. Yield: 0.281 g, 0.351 mmol, 94%. ^1H NMR (δ, ppm in $CDCl_3$): 7.23 (d, 8H, J_{HH} = 8.8 Hz, *Ph*), 6.79 (d, 8H, J_{HH} = 8.8 Hz, *Ph*), 3.80 (s, 12H, $-OCH_3$). ^{13}C NMR (δ, ppm in $CDCl_3$): 177.34 (s), 160.70 (s), 134.64 (s), 130.90, (s), 114.26 (s), 55.86 (s). Absorption spectrum [CH_2Cl_2; λ_{max}, nm (ε_M, M cm^{-1})]: 464 (2990), 860 (52700). Anal. Calcd for $C_{32}H_{28}O_4S_4Pt{\cdot}ClCH_2CH_2Cl$: C, 45.43; H, 3.59; S, 14.27. Found: C, 45.14; H, 3.44; S, 11.99.

[Pt(adt)$_2$(dppe)] ***(6)***. A mixture of solid **5** (0.100 g, 0.125 mmol) and dppe (0.100 g, 0.251 mmol) was dissolved in CH_2Cl_2 (25 mL) to form a deep-blue reaction mixture. The resulting blue solution was stirred vigorously at ambient temperature for 4 h, after which time the solvent was removed under reduced pressure. The residual solid was washed with Et_2O (2 × 10 mL) and then dried under vacuum to afford **6** as a blue solid. Yield: 0.115 g, 0.096 mmol, 77%. ^{31}P NMR (δ, ppm in C_6D_6): 3.01 (s, $^1J_{PtP}$ = 1756.3 Hz). Absorption spectrum [CH_2Cl_2; λ_{max}, nm (ε_M, M cm^{-1})]: 260 (11100), 315 (sh, 32500), 580 (2080).

[Pt(adt)(dppe)] ***(7)***. A vigorously stirred mixture of **5** (0.050 g, 0.063 mmol) and dppe (0.025 g, 0.063 mmol) in 1,2-dichloroethane (15 mL) was heated to 70 °C for 6 h. The deep-blue color formed initially changed to yellow during the course of the reaction. The solvent was removed under pressure, and the solid residue was washed with Et_2O (2 × 10 mL) and dried under vacuum to afford **7** as a yellow solid. Yield: 0.046 g, 0.051 mmol, 82%. ^1H NMR (δ, ppm in CD_2Cl_2): 7.87−7.82 (m, 8H, dppe-*Ph*), 7.49 (br, s, 12H, dppe-*Ph*), 7.07 (d, 4H, J_{HH} = 8.4 Hz, dithiolene-*Ph*), 6.61 (d, 4H, J_{HH} = 8.8 Hz, dithiolene-*Ph*), 3.69 (s, 6H, $-OCH_3$), 2.58−2.48 (m, 4H, dppe $-CH_2$). ^{13}C NMR (δ, ppm in CD_2Cl_2): 133.82 (br, m), 131.35 (s), 128.91 (s), 128.86 (s), 128.81 (s), 112.89 (s), 55.25 (s), 43.67 (s). ^{31}P NMR (δ, ppm in CD_2Cl_2): 45.02 (s, $^1J_{PtP}$ = 2746.73 Hz). Absorption spectrum [CH_2Cl_2; λ_{max}, nm (ε_M, M cm^{-1})]: 330 (43300), 432 (sh, 5000). Anal. Calcd for $C_{42}H_{38}O_2P_2S_2Pt$: C, 56.30; H, 4.27; P, 6.91. Found: C, 54.36; H, 4.39; P, 7.31.

[Pt(adt)$_2$(PMe$_3$)$_2$] ***(8)***. A stirred solution of **5** (0.100 g, 0.125 mmol) in CH_2Cl_2 (20 mL) was treated with PMe_3 in toluene (0.5 mL, 1.0 M solution) delivered via syringe, which induced a change in color from deep red to pale yellow. This reaction mixture was stirred for 24 h at ambient temperature, after which time the solvent was removed under reduced pressure and the resulting solid residue was washed with Et_2O (2 × 10 mL) and dried. Yield: 0.102 g, 0.107 mmol, 86%. ^1H NMR (δ, ppm in CD_2Cl_2): 7.01 (d, 8H, J_{HH} = 8.8 Hz, *Ph*), 6.64 (d, 8H, J_{HH} = 8.8 Hz, *Ph*), 3.71 (s, 12H, $-OCH_3$), 1.81 (t, 18H, J = 4 Hz, $P(CH_3)_3$). ^{13}C NMR (δ, ppm in CD_2Cl_2): 158.54 (s), 135.01 (s), 130.96 (s), 129.95 (s), 113.64 (s), 55.62 (s), 9.24 (t, $P(CH_3)_3$). ^{31}P NMR (δ, ppm in CD_2Cl_2): −18.28 (s, $^1J_{PtP}$ = 1740 Hz). Absorption spectrum [CH_2Cl_2; λ_{max}, nm (ε_M, M cm^{-1})]: 256 (83500), 314 (33900), 428 (sh, 1980). Anal. Calcd for $C_{38}H_{46}O_4P_2S_4Pt$: C, 47.94; H, 4.87; P, 6.51. Found: C, 47.86; H, 4.72; P, 6.45.

[Pt(mdt)$_2$(PMe$_3$)$_2$] ***(9)***. The procedure used in the synthesis of **9** was analogous to that described for **8**. The scale employed for the reaction involved 0.100 g of $[Pt(S_2C_2Me_2)_2]$ (0.232 mmol) and 1.0 mL of PMe_3 in toluene (1.00 mmol). Yield: 0.113 g, 0.194 mmol, 84%. ^1H NMR (δ, ppm in $CDCl_3$): 1.78 (d, 18H, J_{PH} = 13.2 Hz, $P(CH_3)_3$), 1.61 (s, 12H, dithiolene $-CH_3$). ^{13}C NMR (δ, ppm in $CDCl_3$): 122.61 (S, dithiolene *C*=*C*), 21.25 (s, dithiolene $-CH_3$)), 9.24 (t, $P(CH_3)_3$). ^{31}P NMR (δ, ppm in CD_2Cl_2): −19.40, $^1J_{PtP}$ = 1775 Hz). Absorption spectrum [CH_2Cl_2; λ_{max}, nm (ε_M, M cm^{-1})]: 232 (29400), 272 (sh, 7100). Anal. Calcd for $C_{14}H_{30}P_2S_4Pt$: C, 28.80; H, 5.18; P, 10.61. Found: 28.88; H, 5.10; P, 10.85.

[Pd(adt)$_2$] ***(10)***. The procedure employed for the synthesis of **10** was analogous to that used for **5**. The scale on which the reaction was performed involved 0.53 g (1.17 mmol) of **3**, 0.100 g (0.564 mmol) of $PdCl_2$, and 0.143 g (0.563 mmol) of I_2. Yield: 0.359 g, 0.505 mmol, 89%.

[Pd(adt)(PMe$_3$)$_2$] ***(11)***. Trimethylphosphine in toluene (1 M solution, 0.56 mL, 0.56 mmol) was delivered via syringe to a stirring solution of $[Pd(S_2C_2(C_6H_4\text{-}p\text{-}OMe)_2)_2]$ (0.100 g, 0.141 mmol) in CH_2Cl_2 (25 mL) at ambient temperature. The reaction mixture immediately assumed an orange color. Stirring was continued for 12 h, after which time the solvent was removed under reduced pressure and the resulting solid residue was washed with Et_2O (2 × 10 mL) and dried under vacuum. Crystals were grown by the diffusion of hexanes vapor into a C_6H_6 solution. Yield: 0.061 g, 0.109 mmol, 77%. ^1H NMR (δ, ppm in CD_2Cl_2): 7.08 (d, J = 9.2 Hz, 4H, Ph), 6.64 (d, J = 9.2 Hz, 4H, Ph), 3.32 (s, 6H, $-OCH_3$), 1.60 (d, 18H, J_{PH} = 9.2 Hz, $P(CH_3)_3$). ^{13}C NMR (δ, ppm in CD_2Cl_2): 158.19 (s, Ph), 137.20 (s, olefinic C), 134.75 (s, Ph), 131.46 (s, Ph), 128.83 (s, Ph), 113.27 (s, Ph), 55.59 (s, $-OCH_3$), 17.55 (t, $P(CH_3)_3$). ^{31}P NMR (δ, ppm in CD_2Cl_2): −18.49 (s). Absorption spectrum [CH_2Cl_2; λ_{max}, nm (ε_M, M cm^{-1})]: 222 (26700), 266 (44000), 338 (sh, 3560).

[Pd(mdt)(PPh$_3$)$_2$] ***(12)*** *and [Pd$_2$(μ-mdt)$_2$(PPh$_3$)$_2$]* ***(13)***. A portion of $Me_2C_2S_2C{=}O$ (0.063 g, 0.431 mmol) in MeOH (10 mL) was deprotected by the addition of 10% LiOMe in MeOH (0.4 mL, 0.872 mmol). The resulting clear reaction mixture was stirred for 2 h at ambient temperature and then was transferred via a cannula to a Schlenk flask containing *cis*-$[Pd(PPh_3)_2Cl_2]$ (0.305 g, 0.436 mmol) in CH_2Cl_2 (20 mL). The reaction mixture assumed a dark-brown color. Stirring was continued overnight, and the solvent was then removed under reduced pressure. Analysis of the crude product by ^{31}P NMR

dx.doi.org/10.1021/ic501273b | *Inorg. Chem.* 2014, 53, 9192−9205

indicated the presence of two different compounds, which were subsequently separated on a silica column eluted with 1:1 CH_2Cl_2/hexanes. Both compounds were readily crystallized by slow evaporation of the eluant. **12**. Yield: 0.063 g, 0.084 mmol, 19%. R_f: 0.31 (1:1 CH_2Cl_2/hexanes). ^{1}H NMR (δ, ppm in $CDCl_3$): 7.43−7.39 (m, 12H, *Ph*), 7.26 (t, J_{HH} = 8 Hz, 6H, *Ph*), 7.10 (t, J_{HH} = 7.2 Hz, 12H, *Ph*), 1.89 (s, 6H, $-CH_3$). ^{31}P NMR (δ, ppm in $CDCl_3$): 26.40 (s). Absorption spectrum [CH_2Cl_2; λ_{max}, nm (ε_M, M cm^{-1})]: 288 (60000). Anal. Calcd for $C_{40}H_{36}P_2S_2Pd$: C, 64.12; H, 4.84. Found: C, 63.49; H, 4.92. **13**. Yield: 0.070 g, 0.072 mmol, 33%. R_f: 0.17 (1:1 CH_2Cl_2/hexanes). ^{1}H NMR (δ, ppm in $CDCl_3$): 7.67−7.62 (m, 12H, *Ph*), 7.43−7.34 (m, 18H, *Ph*), 1.36 (s, 6H, $-CH_3$), 0.83 (s, 6H, $-CH_3$). ^{13}C NMR (δ, ppm in $CDCl_3$): 135.26 (s), 135.20 (s), 135.14 (s), 130.96 (s), 130.66 (s), 130.51 (s), 128.30 (s), 128.25 (s), 128.19 (s), 115.21 (s), 25.22 (s, $-CH_3$), 21.57 (s, $-CH_3$). ^{31}P NMR (δ, ppm in $CDCl_3$): 32.23 (s). Absorption spectrum [CH_2Cl_2; λ_{max}, nm (ε_M, M cm^{-1})]: 224 (103000), 320 (23500), 420 (12200), 584 (1700). Anal. Calcd for $C_{44}H_{42}P_2S_4Pd_2$: C, 54.26; H, 4.34. Found: C, 54.10; H, 4.44.

RESULTS AND DISCUSSION

Syntheses and Structure. The synthesis of 4,5-di-*p*-anisyl-1,3-dithiol-2-one (**2**; Scheme 1) was undertaken via the acid-

Scheme 1. Synthesis of the *p*-Anisyl-Substituted Dithiolene Ligand

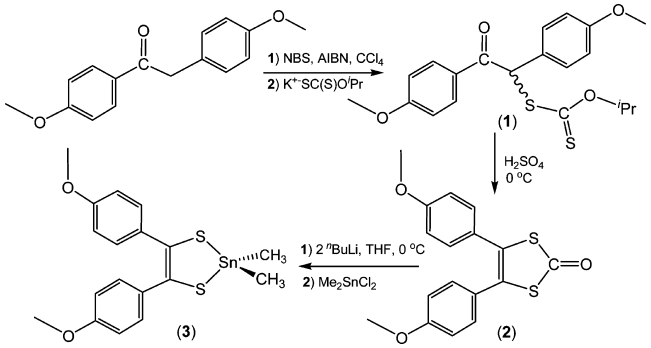

catalyzed cyclization of *O*-isopropyl *rac*-(4-methoxyphenyl-4-methoxyphenacyl)dithiocarbonate (**1**; Scheme 1), a reaction of some generality reported by Bhattacharya and Hortmann.[54] Compound **1** was itself readily obtained in good yield (78%) by an in situ bromination of commercially available desoxyanisoin followed immediately by treatment with potassium *O*-isopropylxanthate. Prepared as a racemic mixture, compound **1** crystallizes as such in centric space group $P2_1/c$ (Table 2); the *S* enantiomer is presented in Figure 1 and shows the syn disposition of the *p*-anisyl groups that is necessary for ring cyclization. Selected bond distances and angles are gathered in Table S1 in the SI. While a fair number of dialkyl dithiocarbonate type molecules have been identified structurally, few of these are compounds in which the dithiocarbonate functionality is positioned α to a carbonyl group. The molecule closest in kind to **1** that has been characterized by X-ray crystallography is (4-pyridyl)C(O)CH_2SC(S)O^{i}Pr.[53]

Compound **2** is a convenient protected form of the dithiolene ligand that is readily unmasked via base hydrolysis and then coordinated to the desired transition complex, usually by the displacement of halide ligands. Bond lengths and angles for **2** (Table S2 in the SI) are similar to those reported for related compounds that have been characterized structurally.[49,55−59] One of the types of metal complexes readily formed from an in situ generated ene-1,2-dithiolate is a dialkyltin dithiolene compound, such as **3** (Scheme 1 and Figure 1). Two

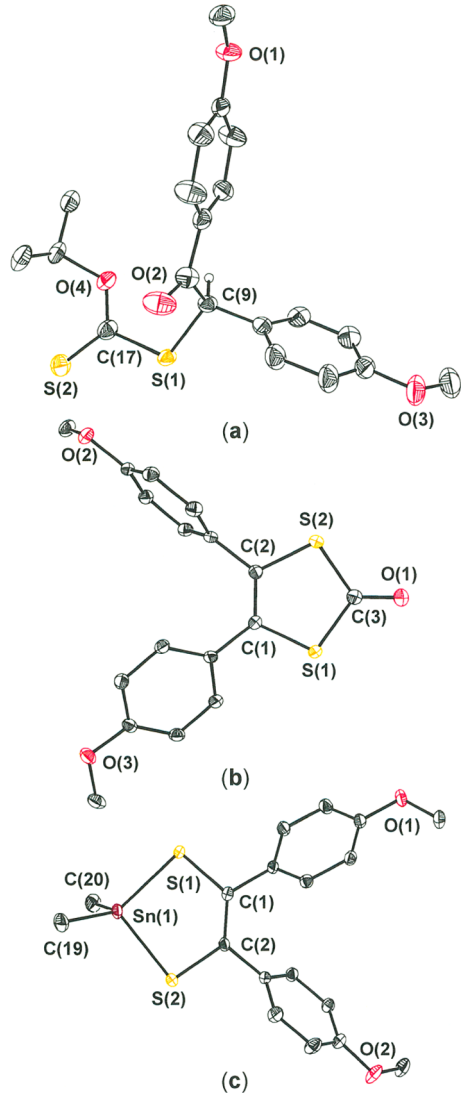

Figure 1. Thermal ellipsoid plots of **1** (a), **2** (b), and **3** (c) at the 50% probability level. Hydrogen atoms are omitted for clarity except for that at the chiral center C(9) in part a.

independent molecules of **3** occur in the asymmetric unit of the cell, one of which is presented in Figure 1, and form relatively close nonbonding intermolecular Sn···S contacts via an offset head-to-head packing arrangement (Figure S17 in the SI). Such intermolecular contacts are typical of this compound type.[60−63] Selected metric parameters for **3** are gathered in Table S3 in the SI and are similar to those observed in related compounds.[49,60−63]

Dialkyltin species such as **3** have utility themselves in transmetalation reactions that afford transition-metal dithiolene complexes and often result in cleaner synthesis compared to reactions employing the alkali-metal ene-1,2-dithiolate salts. Compound **3** and its methyl dithiolene (mdt) variant were thus employed for the preparation of [$M(S_2C_2R_2)_2$] [M = Pt, R = Me (**4**) or *p*-anisyl (**5**); M = Pd, R = *p*-anisyl (**10**)]. We find this synthetic approach (Scheme 2) to be consistent in producing good yields of ∼90% and decidedly preferable to the older P_4S_{10}/acyloin method devised by Schrauzer and Mayweg,[13] at least with these more expensive noble metals. Structural characterization by X-ray crystallography (Figure 2a,b and Tables 2 and 3) revealed idealized D_{2h} point group

dx.doi.org/10.1021/ic501273b | Inorg. Chem. 2014, 53, 9192−9205

Scheme 2. Synthesis of Platinum and Palladium Dithiolenephosphine Complexes

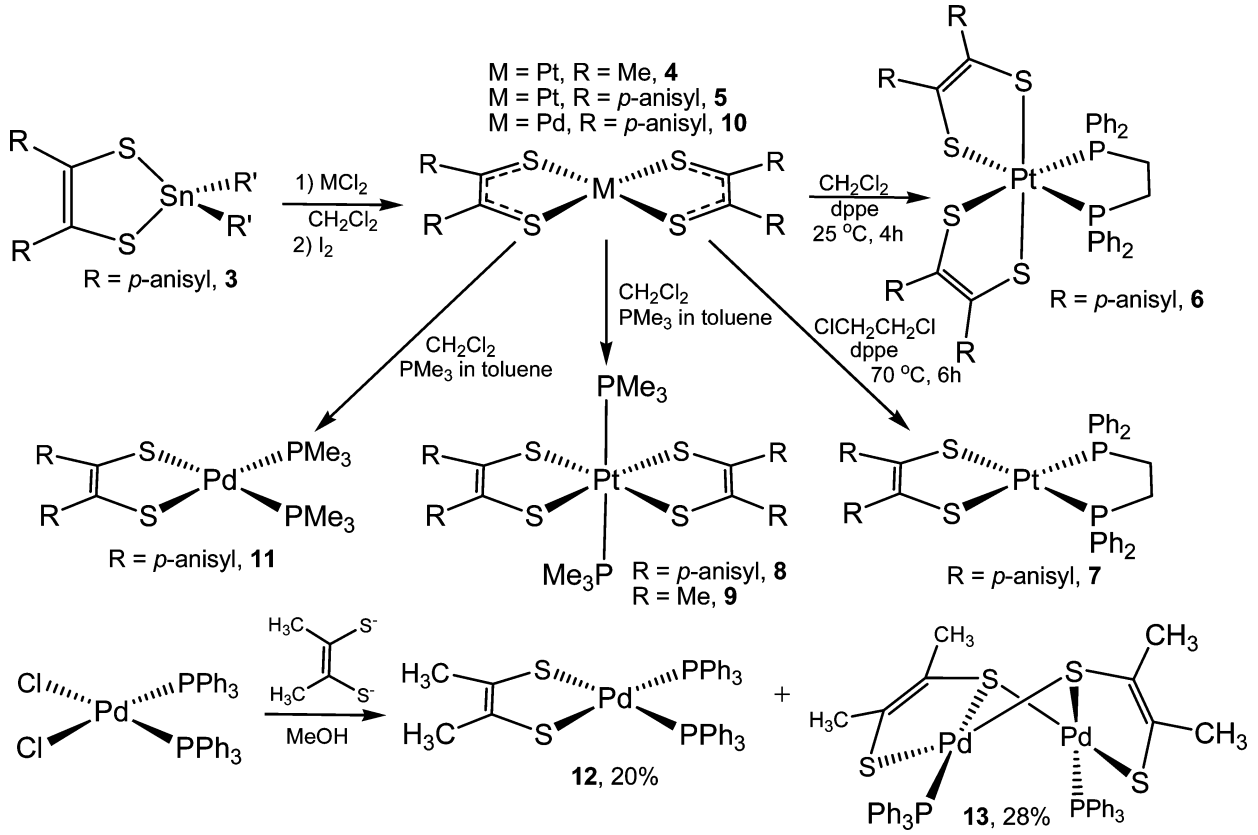

symmetry for **4** but only C_2 symmetry for **5** and **10** owing to the disruption of all mirror planes by the canting angles of the dithiolene *p*-anisyl substituents. An appreciable number of homoleptic platinum and palladium bis(dithiolene) complexes have been identified structurally, although the great majority of these are anionic species with the dicyanoethylene(2−) ligand (mnt^{2-}). Only $[Pt(S_2C_2R_2)_2]$ (R = Ph,[64] *p*-anisyl,[65] *p*-^{t}Bu-C_6H_4,[30] CF_3[66]), $[Pt(dddt)_2]$[67] [dddt = 5,6-dihydro-1,4-dithiin-2,3-dithiolate(2−)], and $[Pt(tmdt)_2]$ [tmdt = trimethylenetetrathiafulvalenedithiolate(2−)][68] are prior examples of mononuclear charge-neutral platinum complexes for which a crystal structure is reported. Crystallographically characterized palladium complexes are fewer still, with $[Pd(norbornylenedithiolate)_2]$[69] and $[Pd(pttdt)_2]$ [pttdt = di-*n*-propylthiotetrathiafulvalenedithiolate(2−)][70] and $[Pd(Et_2timdt)_2]$ (Et_2timdt = monoanion of 1,3-diethylimidazolidine-2,4,5-trithione)[71] being the only precedents. Selected structural parameters for **4**, **5**, and **10** are collected in Table 3 and compared with the corresponding values for $[Ni(mdt)_2]$[72] and $[Ni(adt)_2]$.[73] The similarity of the values confirms the description of **4**, **5**, and **10** as divalent metal ions coordinated by radical monoanions, with the description given for $[Ni(mdt)_2]$ on the basis of detailed structural, S K-edge XAS, and computational studies.[72,75] We note that $[M(adt)_2]^n$ (M = Ni, Pd, Pt) is the only series with $n = 0$ for the group 10 triad for which crystallographic characterization is complete.

The introduction of 2 equiv of PMe_3 or 1 equiv of dppe to CH_2Cl_2 solutions of $[Pt(S_2C_2R_2)_2]$ at ambient temperature cleanly affords the six-coordinate bis(phosphine) adducts (compounds **6**, **8**, and **9**; Scheme 2). The PMe_3 complexes revealed a trans disposition for the phosphine ligands by ^{1}H NMR spectroscopy, a matter subsequently confirmed by X-ray crystallography (Figure 2d), while the related dppe complex has phosphine chelating in the cis fashion, as opposed to bridging between metal atoms in a 1D coordination polymer[76] or cyclic species.[77] Compound **8** (Figure 2d) occurs on a general position in monoclinic $P2_1/n$ but shows only C_i point symmetry, if the staggered arrangement of PMe_3 ligands and the "two down, two up" orientation of the anisyl substituents are considered. Compound **9** crystallizes on a special position in orthorhombic *Cmca* such that the whole molecule is generated from one unique fourth by reflection and inversion operations. The point symmetry in compound **6** is limited to only C_2 rotational symmetry, with the C_2 axis bisecting the S(2)−Pt(1)−S(2A) and P(1)−Pt(1)−P(1A) angles. As noted earlier, compounds **6**, **8**, and **9** are noteworthy as the first such six-coordinate bis(phosphine) adducts of group 10 bis(dithiolene) complexes to be structurally characterized.

Selected averaged bond lengths for **6**, **8**, and **9** are presented in Table 4. Comparison of M−S, S−C, and C−$C_{chelate}$ bond lengths with corresponding values for **4** and **5** in Table 3 shows that the first two bond distances increase, while the third decreases, with the changes being significant within the resolution of the data. The nature and magnitude of these bond-length changes in **6**, **8**, and **9** are indicative of a reduction of the dithiolene ligand from a radical monoanion to fully reduced ene-1,2-dithiolate (Scheme 3b→a). This dithiolene ligand reduction occurs to accommodate the oxidation of Pt^{II} to Pt^{IV}, its typical oxidation state in a six-coordinate octahedral environment. While expansion of a metal's coordination number by association of the phosphine ligands is not usually an oxidative addition reaction, the reactions of **4** and **5** to afford **6**, **8**, and **9** are special cases in which this is so. The reducing equivalents that would normally pass from metal to the species

dx.doi.org/10.1021/ic501273b | Inorg. Chem. 2014, 53, 9192−9205

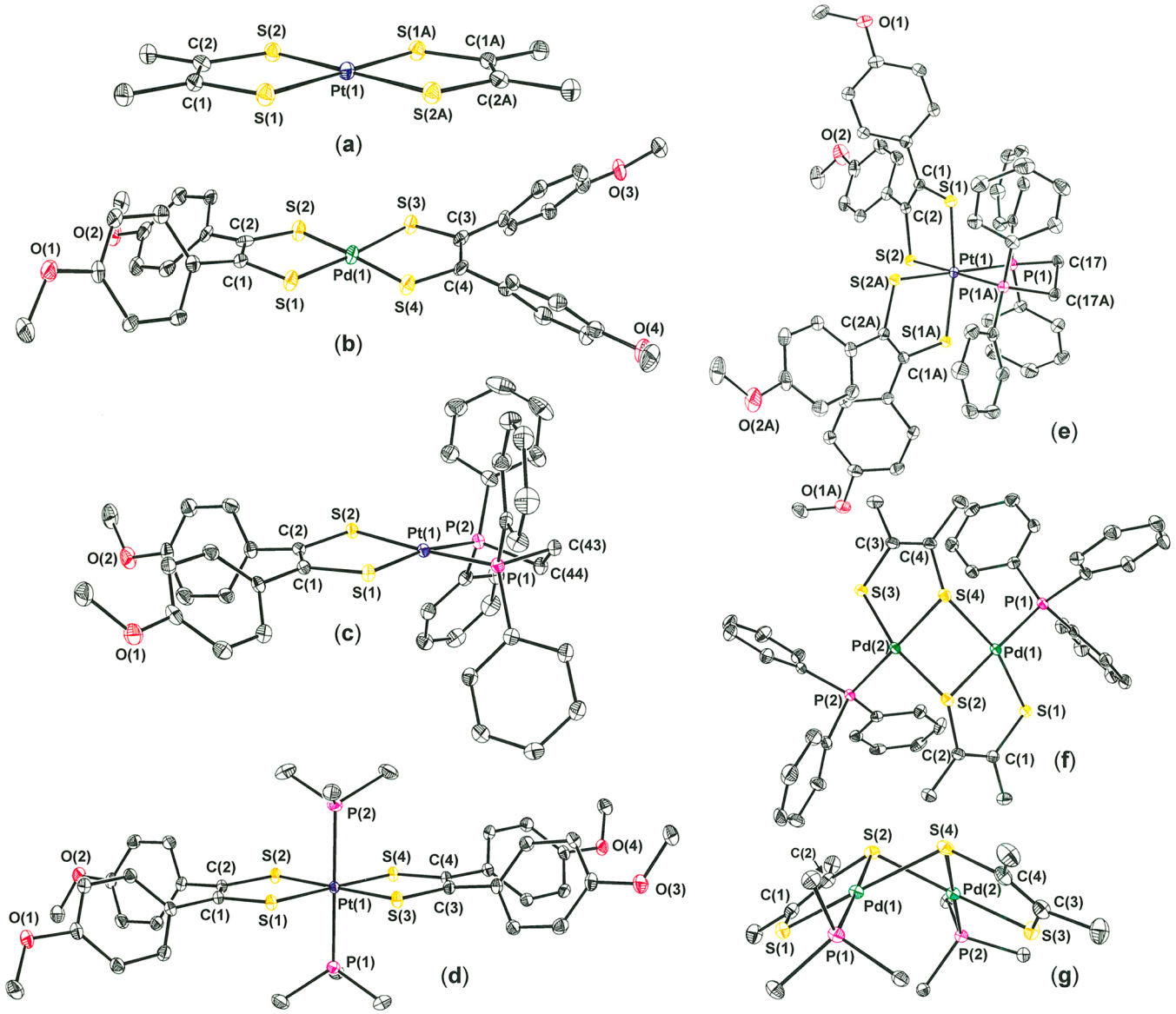

Figure 2. Thermal ellipsoid plots of **4** (a), **10** (b), **7** (c), *trans*-**8** (d), **6** (e), and **13** from top (f) and side (g) views. All hydrogen atoms are omitted for greater clarity.

Table 3. Selected Interatomic Distances (Å) and Angles (deg) for $[M(S_2C_2R_2)_2]$ Complexes[a]

	$[Pt(mdt)_2]$ (**4**)	$[Ni(mdt)_2]$[72]	$[Pt(adt)_2]$ (**5**)	$[Pd(adt)_2]$ (**10**)	$[Ni(adt)_2]$[73]
M–S	2.2550[6]	2.1285[10]	2.244[1]	2.2578[9]	2.1241[3]
S–C	1.705[2]	1.714[4]	1.707[4]	1.708[3]	1.7118[10]
$C–C_{chelate}$	1.388(5)	1.365(9)	1.397[8]	1.414[6]	1.392[2]
$S–M–S_{chelate}$	87.86(3)	88.64(5)	87.68[5]	87.89[4]	91.08[1]
$S–M–S_{cis}$	92.14(3)	91.36(5)	92.41[6]	92.19[4]	89.01[1]
$S–M–S_{trans}$	180.0	180.0	176.65[5]	176.63[5]	176.43[1]
C–S–M	105.37[8]	105.0[1]	106.0[2]	105.8[1]	105.77[4]
C–C–S	120.7[1]	119.4[3]	120.1[3]	120.1[3]	118.56[7]

[a]Chemically identical, crystallographically independent values are averaged. Uncertainties are propagated according to the general formula for uncertainty as a function of several variables, as detailed in ref 74.

that is oxidatively adding are instead transferred to the partially oxidized dithiolene ligands.

Under the same mild conditions as those employed for the synthesis of compound **8**, the analogous six-coordinate diphosphine adduct of palladium complex **10** was not observed. Although probable as an initially formed species, $[Pd(adt)_2(PMe_3)_2]$ is apparently less stable thermally and yields readily to the formation of square-planar C_{2v}-symmetric **11** (Scheme 2). The fate of the substituted dithiolene ligand was not established. The related platinum complex **7** (Scheme 2c and Figure 2) was found to form if the reaction between **5** and dppe was attended by moderate heating (70 °C). Although not

dx.doi.org/10.1021/ic501273b | *Inorg. Chem.* 2014, 53, 9192–9205

Table 4. Selected Interatomic Distances (Å) and Angles (deg) for $[M(S_2C_2R_2)_2]$ Complexes[a]

	$[M(S_2C_2R_2)_2(PR'_3)_2]$			$[M(S_2C_2R_2)(PR'_3)_2]$		
	6	8	9	7	11	12
M–S	2.3654(5),[b] 2.3688(5)[c]	2.3656[3]	2.3619(8)	2.2923[4]	2.2918[3]	2.2922[3]
M–P	2.3376(6)	2.3597[4]	2.3625(12)	2.2586[4]	2.3054[3]	2.3142[3]
S–C	1.762(2),[b] 1.776(2)[c]	1.7683[10]	1.769(4)	1.764[2]	1.7627[11]	1.7639[12]
$C–C_{chelate}$	1.356(3)	1.343[2]	1.345(7)	1.347[3]	1.353(2)	1.335(2)
$S–M–S_{chelate}$	88.085(19)	88.468[12]	88.27(4)	87.95[2]	87.124(13)	87.341(14)
$S–M–S_{cis}$	86.189(19),[b] 93.65(3)[c]	91.535[12]	91.73(4)			
$S–M–S_{trans}$	171.63(3)	179.428[12]	180.0			
P–M–P	86.41(3)	179.437(18)	180.0	86.18[2]	96.368(16)	97.605(14)
$P–M–S_{cis}$	92.38(2),[b] 89.995(19)[c]	89.999[7]	90.00[2]	93.17[2]	88.303[11]	88.804[10]
$P–M–S_{trans}$	176.035(19)			174.24[2]	174.681[11]	166.651[10]
C–S–M	102.35(8),[b] 102.94(7)[c]	102.11[4]	102.53(12)	104.50[5]	105.62[4]	104.65[4]
C–C–S	124.46(17),[b] 121.49(16)[c]	123.61[7]	123.32(12)	121.4[1]	120.81[8]	121.23[8]

[a]Chemically identical, crystallographically independent values are averaged. Uncertainties are propagated according to the general formula for uncertainty as a function of several variables, as detailed in ref 74. [b]Bond length/angle involving S(1). [c]Bond length/angle involving S(2).

Scheme 3. Redox Levels for a Dithiolene Ligand with Typical C–S and C–C Bond Lengths Indicated

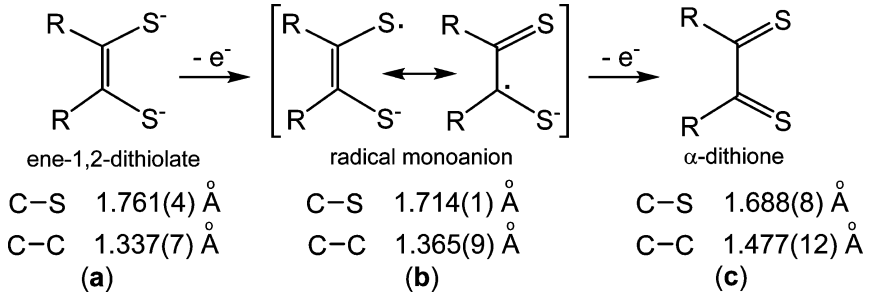

confirmed in a deliberate experiment, these observations suggest strongly that solutions of **6** would lead to **7** if subjected to the same temperature for a similar duration of time.

The obvious approach to the synthesis of $[M(S_2C_2R_2)(PR'_3)_2]$ via halide displacement from $[MCl_2(PR'_3)_2]$ by an ene-1,2-dithiolate salt was examined with in situ generated Li_2(mdt) and $[PdCl_2(PPh_3)_2]$. The anticipated **12** (Scheme 2) was isolated in a modest yield of 19% along with a comparable amount (33%) of the dipalladium species $[(Ph_3P)Pd(\mu\text{-mdt})_2Pd(PPh_3)]$ (**13**; Scheme 2). Dinuclear compound **13** is of a type first prepared by Mayweg and Schrauzer,[15] although the specific nature of the dimerically formulated compound was not then established. Compound **13** shows square-planar palladium(II) centers, with each metal ion coordinated by a single PPh_3 ligand and chelated by a single mdt ligand, one sulfur atom of which forms a bridge to the other palladium(II) ion (Figure 2f). The two square-planar palladium(II) centers are thus hinged by two bridging thiolate-type sulfur atoms and form a dihedral angle of 73.4° along the S(2)···S(4) interatomic axis (Figure 2g). The S–C and $C–C_{chelate}$ bond lengths in the mdt ligands are indicative of a fully reduced ene-1,2-dithiolate ligand (Table 5). The bridging is asymmetric, with the bridging sulfur atom being ∼0.036 Å nearer to the palladium ion to which the other sulfur atom of the same ligand is bound. Although it occurs on a general position in $P\bar{1}$, **13** shows C_2 point group symmetry overall.

We note a recent report of closely related $[(Ph_3P)Pd(\mu\text{-}1,2\text{-ethylenedithiolato-}S,S':S)_2Pd(PPh_3)]$,[78] which was formed in a serendipitous reaction between $[Pd(PPh_3)_4]$ and tetrathiafulvalene. This compound is isostructural to **13** but differs crystallographically by occurring on a 2-fold rotation axis in

Table 5. Selected Interatomic Distances (Å) and Angles (deg) for 13[a]

Pd···Pd	2.9650(2)	$S–Pd–S_{chelate}$	87.654[11]
$Pd–S_{nonbridging}$	2.2816[3]	$S_{bridging}–Pd–S_{bridging}$	78.621[10]
$Pd–S_{br,short}$	2.3171[3]	$S–Pd–S_{trans}$	165.315[11]
$Pd–S_{br,long}$	2.3844[3]	$P–Pd–S_{bridging,cis}$	102.588[10]
Pd–P	2.2857[3]	$P–Pd–S_{bridging,trans}$	177.553[11]
$S–C_{bridging}$	1.7730[12]	$P–Pd–S_{nonbridging,cis}$	91.151[11]
$S–C_{nonbridging}$	1.7574[12]	Pd–S–Pd	78.181[9]
$C–C_{chelate}$	1.344[1]	θ[b]	73.9

[a]Chemically identical, crystallographically independent values are averaged. Uncertainties are propagated according to the general formula for uncertainty as a function of several variables as detailed in ref 74. [b]Fold angle between mean PdS_3P planes.

*C*2/*c*.[79] The same folded butterfly motif occurs with $[(Ph_3P)Pd(\mu\text{-}1,2\text{-ethanedithiolato-}S,S':S)_2Pd(PPh_3)]$,[80] in which the dithiolate ligand is fully reduced, but fully planar or nearly planar $Pd(\mu\text{-}S)_2Pd$ core structures are typical for related complexes bearing monodendate thiolate ligands, such as $[(Ph_3P)(SPh)Pd(\mu\text{-}SPh)_2Pd(SPh)(PPh_3)]$,[81] $[(Ph_3P)(SC_6F_5)Pd(\mu\text{-}SC_6F_5)_2Pd(SC_6F_5)(PPh_3)]$,[82−84] and $[((^iPrO)_3P)(SPh)Pd(\mu\text{-}SPh)_2Pd(SPh)((P(O^iPr)_3)]$.[85] It is likely that the folded $Pd(\mu\text{-}S)_2Pd$ core seen in **13** and in $[(Ph_3P)Pd(\mu\text{-}1,2\text{-ethylenedithiolato-}S,S':S)_2Pd(PPh_3)]$ is a consequence of the restricted intraligand S–S separation imposed by the chelating ligand. The intraligand distances between terminal and bridging sulfur atoms in **13** average to 3.185 Å, somewhat less than the corresponding distance of 3.389 Å found, for example, in $[(Ph_3P)(SPh)Pd(\mu\text{-}SPh)_2Pd(SPh)(PPh_3)]$.[81] We note that the interpalladium separation of 2.9650(2) Å is substantially shorter

dx.doi.org/10.1021/ic501273b | Inorg. Chem. 2014, 53, 9192−9205

than twice the van der Waals radius of this element (3.26 Å)[86] and close enough to support potential interaction between the two ions.

Electrochemistry. The cyclic voltammetry for bis-(dithiolene) complex **5**, shown in Figure 3, reveals two

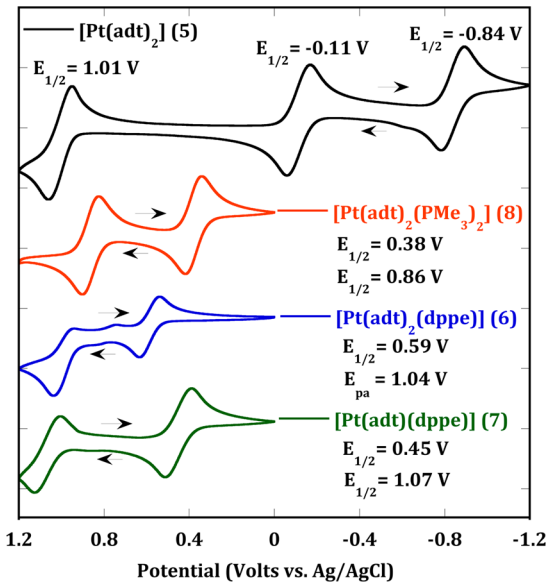

Figure 3. Cyclic voltammetry for **5**–**8** in CH_2Cl_2 recorded with $[^nBu_4N][PF_6]$ as the supporting electrolyte at 25 °C (−78 °C for **6** with a scan rate of 100 mV·s^{-1}.

reversible reductions at $E_{1/2}$ = −0.11 and −0.84 V and a single reversible oxidation at $E_{1/2}$ = +1.01 V. The similarity of these redox features with corresponding reductions and an oxidation for $[Ni(adt)_2]$ and **10** (Figures S18 and S19 in the SI) supports their assignment as dithiolene-ligand-based processes in which the metal remains in an invariant M^{II} divalent state. This interpretation is affirmed by inspection of the frontier molecular orbitals (MOs) of **5** following a geometry optimization, which shows both the highest occupied molecular orbital (HOMO) and lowest unoccupied molecular orbital (LUMO) to be largely comprised of the dithiolene C_2S_2 π system (vide infra; Figure S28 in the SI), although the latter does have a modest degree of metal d character.

The cyclic voltammogram for **8** shows reversible oxidations at +0.38 and +0.86 V, which are assigned as successive oxidations of the two dithiolene ligands, with platinum being already at a high oxidation level (Pt^{IV}) and the dithiolene ligands being fully reduced, as indicated by the crystallographic data (vide supra). The voltammogram for **6** displays two oxidation features, the first being a reversible oxidation at +0.59 V and the second an irreversible process at ∼+1.04 V. The potential for the first oxidation of **6** is ∼0.2 V more positive than the first oxidation for **8**, a difference attributable to the greater basicity of the PMe_3 ligand. What effect the cis arrangement of the phosphine ligand has on the electrochemistry of **6**, as opposed to the trans configuration as found in **8**, is unclear but is presumably slight. In **7**, the presence of only oxidation features, the first of which (at +0.45 V) is fully reversible, and the absence of any reduction processes are consistent with the compound being composed of fully reduced ene-1,2-dithiolate ligands and a divalent metal ion, neither of which is capable of further reduction. Both oxidations in **7** are attributed to the adt ligand, the second of which creates the fully oxidized α-dithione form (Scheme 3c). The full range of dithiolene redox levels has also been observed electrochemically in the related complexes [(adt)M(μ-tpbz)M(adt)] [M = Ni, Pd, Pt; tpbz = 1,2,4,5-tetrakis(diphenylphosphino)benzene].[87]

UV–Vis and XAS. The UV–vis spectra of **5** and of the phosphine complexes **6**–**8** are presented in Figure 4. The

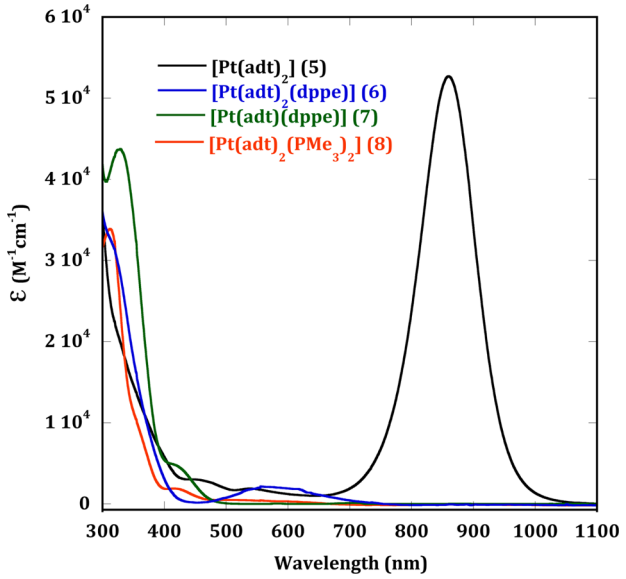

Figure 4. UV–vis spectra (CH_2Cl_2, 25 °C) for **5**–**8**.

arresting feature in the spectrum of **5** is the low-energy intense absorption band at 860 nm, a ligand-to-ligand charge-transfer (LLCT) transition and well-known spectroscopic marker for the presence of π-radical monoanionic dithiolene ligands (Scheme 3b). In the spectra of all of the phosphine adducts, this absorption is conspicuously absent, which confirms the crystallographic interpretation of fully reduced ene-1,2-dithiolates coordinated to platinum (Scheme 3a). The spectrum for **6** shows a broad band of low intensity at 580 nm, which does not have a counterpart in the spectrum of **8**. Although an assignment for this transition has not been attempted with computational assistance, it is probable that it appears in **6** and not **8** because of the lack of inversion symmetry and differently constituted and ordered frontier MOs in the former. Complex **4** shows a LLCT absorption at 739 nm, which accords with the ordering of ligand substituent influences previously tabulated for nickel bis(dithiolene) complexes.[5]

To assist the description of the redox levels of the dithiolene ligand and platinum metal in compounds **5**–**8**, both S K-edge and Pt L_1-edge XAS spectra were obtained, the results of which are presented in Figure 5. The energies of the pre-edge absorption maxima, which were determined after a pseudo-Voigt deconvolution of overlapping features in the pre-edge region (Figures S20–S23 in the SI), are given in Table 6. These pre-edge absorptions in the S K-edge X-ray spectra arise from transitions from S 1s orbitals to acceptor MOs bearing S p character and manifest intensity according to the degree of their S p character.[88] Rising-edge energies in both the S K-edge and Pt L_1-edge XAS were identified as the inflection points in the second derivatives of the XAS spectra in the rising-edge region (Figures S24–S27 in the SI).

The S K-rising-edge energy for **5** at 2473.8 eV is ∼1.3 eV higher in energy than that for **6** and **8**, which is consistent with

dx.doi.org/10.1021/ic501273b | Inorg. Chem. 2014, 53, 9192–9205

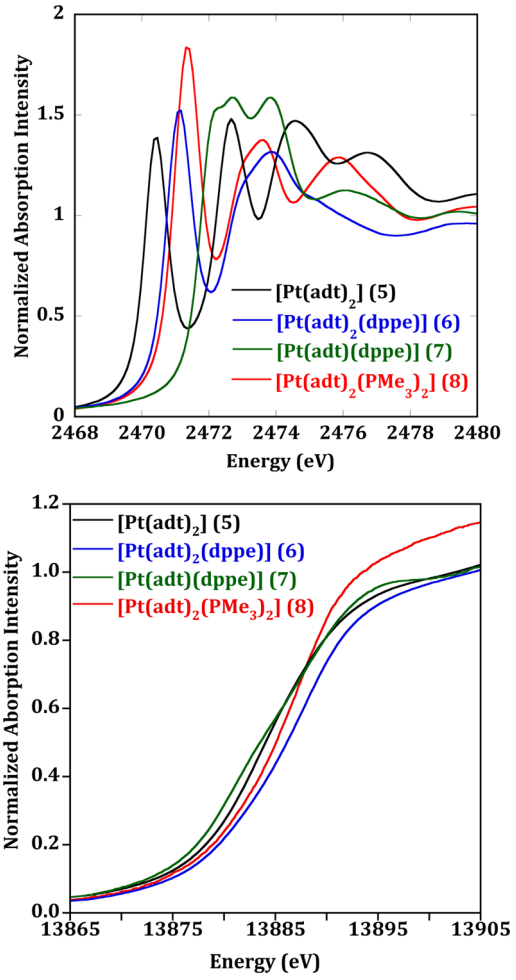

Figure 5. Normalized S K-edge (top panel) and Pt L_1-edge (bottom panel) XAS spectra for **5**–**8**.

Table 6. S K-Pre-edge, S K-Edge, and Pt L_1-Edge Energies (eV) for 5–8

	S K-pre-edge S 1s → LUMO		S K-edge (eV)	Pt L_1-edge (eV)
compound	energy (eV)	intensity	S 1s → 4p	Pt 2s → 6p
$[Pt(adt)_2]$ (**5**)	2470.3	1.30	2473.8	13878.9
	2472.5	1.46		
$[Pt(adt)_2(dppe)]$ (**6**)	2471.0	1.51	2472.5	13880.1
[Pt(adt)(dppe)] (**7**)	2471.9	0.70	2473.5	13877.9
	2472.7	0.41		
$[Pt(adt)_2(PMe_3)_2]$ (**8**)	2471.2	1.83	2472.5	13879.8

the partially oxidized (radical) character of its dithiolene ligands, compared to the fully reduced ene-1,2-dithiolate ligands indicated for **6**–**8** on the foregoing combined evidence of crystallography, electrochemistry, and UV–vis absorption spectroscopy. The lowest-energy pre-edge feature for **5** at 2470.3 eV is a S 1s → LUMO transition (Table 6), which owes its intensity to the substantial S p character in the acceptor MO (Figure S28 in the SI). This kind of low-energy pre-edge excitation in the S K-edge XAS is diagnostic of the presence of a dithiolene ligand with radical monoanionic character. The higher-energy pre-edge transition for **5**, at 2472.5 eV, is of an intensity comparable to the lower-energy feature and assigned, from inspection of the LUMOs, as a S 1s → LUMO+1 excitation. Composed of the Pt $d_{x^2-y^2}$ and four S p orbitals in σ^* combination (Figure S28 in the SI), the LUMO+1 is the only other nearby unoccupied MO with appreciable S p character. Related $[(M(dithiolene)_2]^z$ complexes have been interrogated spectroscopically by S K-edge XAS and analyzed computationally in considerable detail (M = Ni; dithiolene = mdt; z = 0, 1−, 2−;[75] M = Ni, dithiolene = mnt, z = 1−, 2−;[89] M = Ni, Pd or Pt, dithiolene = bdt, z = 1−, 2−;[90] M = Ni, Pd, or Pt, dithiolene = 3,5-di-*tert*-butylbenzenedithiolate, z = 0, 1−, 2−).[91] The nature and intensity of the two pre-edge transitions in the S K-edge spectrum of **5** are essentially identical with those described for the charge-neutral $[(M(dithiolene)_2]^z$ complexes noted in the studies above.

To assist a definitive assignment of the pre-edge transitions in their S K-edge XAS spectra, the geometries of **6** and **8** were optimized. The LUMO and LUMO+1 for these compounds, both possible acceptor orbitals for these transitions, are presented in Figure 6, while Table 7 summarizes the

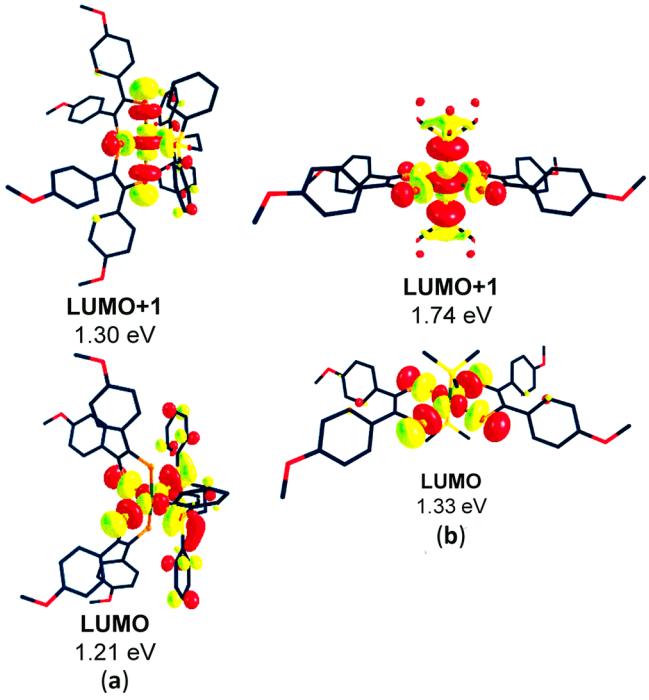

Figure 6. Images of the LUMO and LUMO+1 for **6** (a) and **8** (b) drawn at the 0.035 contour level. Energies are relative to the HOMO (not shown).

contributions of the Pt d and S p atomic orbitals to their composition, as given by a Loewdin orbital population analysis. The LUMOs of both **6** and **8** are of similar description, being σ^* in nature between the metal $d_{x^2-y^2}$ and ligand p orbitals. The LUMO for **8** differs from that of **6** in that its p orbital contributions arise only from sulfur, whereas the latter has both P p and S p character. The greater S p character to the LUMO versus LUMO+1 for both **6** and **8** identifies it as the more likely acceptor orbital for the lowest-energy pre-edge transition (Figures S29 and S30 in the SI and Table 7). This assignment is confirmed by time-dependent density functional theory (TD-DFT) simulation of these excitations (Figure S32 in the SI). The rising edges for both **6** and **8** show unresolved additional feature(s) that may arise from, at least in part, transitions to the

dx.doi.org/10.1021/ic501273b | *Inorg. Chem.* 2014, 53, 9192–9205

Table 7. Composition of Frontier MOs for 5−8

	[Pt(adt)$_2$] (5)		[Pt(adt)$_2$(dppe)] (6)		[Pt(adt)(dppe)] (7)		[Pt(adt)$_2$(PMe$_3$)$_2$] (8)	
	% Pt d	% S p	% Pt d	% S p	% Pt d	% S p	% Pt d	% S p
HOMO	0.4	16.6	4.6	44.3	3.0	32.2	8.0	49.4
LUMO	14.3	46.8	1.3	52.8	13.2	9.6	31.8	40.0
LUMO+1	30.8	32.9	22.4	19.9	3.0	1.1	33.3	17.4

LUMO+1 because both of these orbitals are constituted with a moderate degree of S p character. Compound **7**, in contrast to **6** and **8**, shows no well-resolved pre-edge transitions at ∼2471 eV but rather higher-energy features at ∼2471.9 and 2472.7 eV that overlap with the rising edge. Inspection of the frontier MOs for **7** (Figure S31 in the SI and Table 7) identifies the LUMO again as the empty orbital most suited by virtue of S p character to serve as an acceptor MO. Although more complicated by having substantial contribution from the dppe ligand, the LUMO in **7** has some similarity to those of **6** and **8** in having σ^* character between the S p and Pt $d_{x^2-y^2}$ orbitals. TD-DFT simulations affirm that excitation to the LUMO of **7** is the first and most important contribution to its pre-edge features in the S K-edge XAS spectrum (Figure S32 in the SI).

The effective nuclear charge at platinum, Z_{eff}, can be gauged in a direct way from the Pt L_1-edges, which have their basis in electric-dipole-allowed Pt 2s → 6p transitions. The platinum(II) species **5** and **7** exhibit rising-edge energies of 13878.9 and 13877.9 eV, respectively, whereas octahedral **6** and *trans*-**8** show rising-edge energies that are positively shifted to higher energy at 13880.1 and 13879.8 eV. Qualitatively, the higher rising-edge energies for **6** and **8** are consistent with their formulation as platinum(IV) species, as suggested by the appearance of fully reduced dithiolene ligands in their crystal structures and as expected for six-coordinate octahedral platinum. In measurements of W L_1-edge XAS spectra of a variety of six-coordinate compounds, a change of ∼0.5 eV suggested itself as a typical energy change for a third-row metal L_1-rising-edge energy upon a change of metal formal oxidation state by one unit.[92] The difference of ∼1.0 eV in the rising-edge energies for **5** versus **6** and **8** is consistent with this observation but may be simply fortuitous. Differing ligand-field effects arising from the different coordination numbers and geometries for **5** and **7** versus **6** and **8** complicate the comparison of Pt L_1-rising-edge energies between the two sets and may contribute to the greater difference of ∼2.0 eV seen for **7** versus **6** and **8**.

SUMMARY AND CONCLUSIONS

In this contribution, we have reported high-yielding syntheses of **4** and **5** via transmetalation reactions with $R'_2Sn(S_2C_2R_2)$ (R = Me, $-C_6H_4$-*p*-OCH_3) complexes. Bis(phosphine) adducts of these platinum complexes have been prepared and characterized spectroscopically, electrochemically, and structurally by X-ray diffraction. These six-coordinate complexes display octahedral geometries, a noteworthy contrast with trigonal-prismatic $[W(S_2C_2Me_2)_2(PMe_3)_2]$ and $[W(S_2C_2Me_2)_2(dppe)]$. The dithiolene ligand C−S and $C-C_{chelate}$ bond lengths, as determined crystallographically, are indicative of fully reduced ene-1,2-dithiolates in all phosphine adducts, both for six-coordinate $[Pt(S_2C_2R_2)_2(phosphine)_2]$ and four-coordinate $[Pt(S_2C_2R_2)(phosphine)_2]$ complexes. The UV−vis spectra of these complexes corroborate this interpretation. Thus, the coordination of two phosphine ligands to $[Pt^{II}(adt)_2]$ occasions an internal metal-to-ligand charge transfer, $[Pt^{II}(adt^{\bullet-})_2]$ + $2PR_3$ → $[Pt^{IV}(adt^{2-})_2(PR_3)_2]$, such that the expanded ligand set can be accommodated.

In their report reaffirming their claim of the synthesis of $[Pt(S_2C_2R_2)_2(phosphine)_2]$ compounds,[15] Mayweg and Schrauzer noted the pronounced differences in their electronic absorption and vibrational spectra compared to those of the homoleptic bis(dithiolene) precursors. Although the ideas and associated language of ligand redox noninnocence were undeveloped at that time, they correctly attributed these observations to an alteration of the dithiolene ligands from a delocalized electronic description and commented on the useful insight into these compounds that X-ray crystal structures would offer. A surprising 48 years after Mayweg and Schrauzer's work, this report shows through a combination of crystallography, cyclic voltammetry measurements, and spectroscopic characterization by UV−vis and XAS that phosphine association to $[Pt(S_2C_2R_2)_2]$, which is generally not a redox process, can in this case be described as oxidative addition. This behavior is an example of dithiolene redox noninnocence that is distinctly different from the other manifestations of the phenomenon that we have recently noted, such as variations in dithiolene reduction in formally isoelectronic complexes as a function of ancillary ligands[93] and internal metal dithiolene redox reorganization induced by a coordination geometry change.[94] Because the $[Pt^{II}(adt^{\bullet-})_2]$ + $2PR_3$ → $[Pt^{IV}(adt^{2-})_2(PR_3)_2]$ reaction that is highlighted in this report involves internal redox reorganization between a metal and a ligand in a net nonredox process, it is necessarily an instance of redox innocence involving the combination of both a metal and a ligand, as opposed to a ligand alone, as discussed by Ward and McCleverty.[95]

ASSOCIATED CONTENT

Supporting Information

Full description of procedures for crystal growth, diffraction data collection and processing, and structure solution and refinement, complete crystallographic data for all new structures in CIF format, thermal ellipsoid plots with complete atom labeling, tables of selected bond lengths and angles for compounds **1**−**3**, Figures S1−S32, and description of computational methods and coordinates for geometry-optimized structures. This material is available free of charge via the Internet at http://pubs.acs.org.

AUTHOR INFORMATION

Corresponding Authors

*E-mail: chandru@lamar.edu.
*E-mail: donahue@tulane.edu.

Notes

The authors declare no competing financial interest.

ACKNOWLEDGMENTS

The Louisiana Board of Regents is thanked for enhancement Grant LEQSF-(2002-03)-ENH-TR-67, with which Tulane's X-

ray diffractometer was purchased, and Tulane University is acknowledged for its ongoing support with operational costs for the diffraction facility. Support from the National Science Foundation (Grant CHE-0845829 to J.P.D.) and from the Georges Lurcy Grant and Tulane Provost Fund for Undergraduate Research (to S.C.) is gratefully acknowledged. Use of the SSRL, SLAC National Accelerator Laboratory, is supported by the U.S. Department of Energy, Office of Science, Office of Basic Energy Sciences, under Contract DE-AC02-76SF00515.

REFERENCES

(1) McNamara, W. R.; Han, Z.; Yin, C.-J.; Brennessel, W. W.; Holland, P. L.; Eisenberg, R. *Proc. Natl. Acad. Sci. U.S.A.* **2012**, *109*, 15594−15595.
(2) Faulmann, C.; Cassoux, P. *Prog. Inorg. Chem.* **2004**, *52*, 399−490.
(3) Pilato, R. S.; van Houten, K. A. *Prog. Inorg. Chem.* **2004**, *52*, 369−398.
(4) Cummings, S. D.; Eisenberg, R. *Prog. Inorg. Chem.* **2004**, *52*, 315−368.
(5) Mueller-Westerhoff, U. T.; Vance, B.; Yoon, D. I. *Tetrahedron* **1991**, *47*, 909−932.
(6) Robertson, N.; Cronin, L. *Coord. Chem. Rev.* **2002**, *227*, 93−127.
(7) Cassoux, P.; Valade, L.; Kobayashi, H.; Kobayashi, A.; Clark, R. A.; Underhill, A. E. *Coord. Chem. Rev.* **1991**, *110*, 115−160.
(8) Enemark, J. H.; Cooney, J. J. A.; Wang, J.-J.; Holm, R. H. *Chem. Rev.* **2004**, *104*, 1175−1200.
(9) Zarkadoulas, A.; Koutsouri, E.; Mitsopoulou, C. A. *Coord. Chem. Rev.* **2012**, *256*, 2424−2434.
(10) Geary, E. A. M.; McCall, K. L.; Turner, A.; Murray, P. R.; McInnes, E. J. L.; Jack, L. A.; Yellowlees, L. J.; Robertson, N. *Dalton Trans.* **2008**, *28*, 3701−3708.
(11) Cocker, T. M.; Bachman, R. E. *Inorg. Chem.* **2001**, *40*, 1550−1556.
(12) Davison, A.; Edelstein, N.; Holm, R. H.; Maki, A. H. *Inorg. Chem.* **1964**, *3*, 814−823.
(13) Schrauzer, G. N.; Mayweg, V. P. *J. Am. Chem. Soc.* **1965**, *87*, 1483−1489.
(14) Davison, A.; Howe, D. V. *Chem. Commun.* **1965**, 290−291.
(15) Mayweg, V. P.; Schrauzer, G. N. *Chem. Commun.* **1966**, 640−641.
(16) Bowmaker, G. A.; Boyd, P. D. W.; Campbell, G. K. *Inorg. Chem.* **1983**, *22*, 1208−1213.
(17) Nomura, M.; Okuyama, R.; Fujita-Takayama, C.; Kajitani, M. *Organometallics* **2005**, *24*, 5110−5115.
(18) Bevilacqua, J. M.; Zuleta, J. A.; Eisenberg, R. *Inorg. Chem.* **1994**, *33*, 258−266.
(19) Landis, K. G.; Hunter, A. D.; Wagner, T. R.; Curtin, L. S.; Filler, F. L.; Jansen-Varnum, S. A. *Inorg. Chim. Acta* **1998**, *282*, 155−162.
(20) Johnson, C. E.; Eisenberg, R.; Evans, T. R.; Burberry, M. S. *J. Am. Chem. Soc.* **1983**, *105*, 1795−1802.
(21) Keefer, C. E.; Bereman, R. D.; Purrington, S. T.; Knight, B. W.; Boyle, P. D. *Inorg. Chem.* **1999**, *38*, 2294−2302.
(22) Fitzmaurice, J. C.; Slawin, A. M. Z.; Williams, D. J.; Woollins, J. D.; Lindsay, A. J. *Polyhedron* **1990**, *9*, 1561−1565.
(23) Foguet, R.; Sampedro, F.; Ortiz, J. A.; Cayuela, S.; Castello, J. M.; De Andres, L.; Bonal, J. Eur. Pat. Appl.EP 258655 A2 19880309, 1988.
(24) Hunt, S. W.; Wang, X.; Richmond, M. G. *J. Mol. Struct.* **2009**, *919*, 34−40.
(25) Poola, B.; Hunt, S. W.; Wang, X.; Richmond, M. G. *Polyhedron* **2008**, *27*, 3693−3699.
(26) Sato, M.; Sensui, M.-A. *J. Organomet. Chem.* **1997**, *538*, 1−8.
(27) Dudis, D. S.; King, C.; Fackler, J. P., Jr. *Inorg. Chim. Acta* **1991**, *181*, 99−102.
(28) Ford, S.; Lewtas, M. R.; Morley, C. P.; Di Vaira, M. *Eur. J. Inorg. Chem.* **2000**, 933−938.
(29) Bevilacqua, J. M.; Eisenberg, R. *Inorg. Chem.* **1994**, *33*, 2913−2923.
(30) Pap, J. S.; Benedito, F. L.; Bothe, E.; Bill, E.; DeBeer George, S.; Weyhermüller, T.; Wieghardt, K. *Inorg. Chem.* **2007**, *46*, 4187−4196.
(31) Kaiwar, S. P.; Hsu, J. K.; Liable-Sands, L. M.; Rheingold, A. L.; Pilato, R. S. *Inorg. Chem.* **1997**, *36*, 4234−4240.
(32) Kaiwar, S. P.; Vodacek, A.; Blough, N. V.; Pilato, R. S. *J. Am. Chem. Soc.* **1997**, *119*, 3311−3316.
(33) Keefer, C. E.; Purrington, S. T.; Bereman, R. D.; Knight, B. W.; Bedgood, D. R., Jr.; Boyle, P. D. *Inorg. Chim. Acta* **1998**, *282*, 200−208.
(34) Vicente, R.; Ribas, J.; Cassoux, P. *Nouv. J. Chim.* **1984**, *8*, 653−658.
(35) Vicente, R.; Ribas, J.; Solans, X.; Font-Altaba, M.; Mari, A.; De Loth, P.; Cassoux, P. *Inorg. Chim. Acta* **1987**, *132*, 229−236.
(36) Guyon, F.; Knorr, M.; Garillon, A.; Strohmann, C. *Eur. J. Inorg. Chem.* **2012**, 282−291.
(37) Shin, K.-S.; Jung, Y.-J; Lee, S.-K.; Fourmigué, M.; Barrière, F.; Bergamini, J.-F.; Noh, D.-Y. *Dalton Trans.* **2008**, 5869−5871.
(38) Noh, D.-Y.; Seo, E.-M.; Lee, H.-J.; Jang, H.-Y.; Choi, M.-G.; Kim, Y. H.; Hong, J. *Polyhedron* **2001**, *20*, 1939−1945.
(39) Nakajima, Y.; Nakatani, M.; Hayashi, K.; Shiraishi, Y.; Takita, R.; Okazaki, M.; Ozawa, F. *New J. Chem.* **2010**, *34*, 1713−1722.
(40) Lee, S.-K.; Shin, K.-S.; Noh, D.-Y.; Jeannin, O.; Barrière, F.; Bergamini, J.-F.; Fourmigué, M. *Chem.—Asian J.* **2010**, *5*, 169−176.
(41) Lesley, M. J. G.; Clegg, W.; Marder, T. B.; Norman, N. C.; Orpen, A. G.; Scott, A. J.; Starbuck, J. *Acta Crystallogr., Sect. C* **1999**, *55*, 1272−1275.
(42) Maisela, L. L.; Crouch, A. M.; Darkwa, J.; Guzei, I. A. *Polyhedron* **2001**, *20*, 3189−3200.
(43) Berenguer, J. R.; Bernechea, M.; Forniés, J.; García, A.; Lalinde, E.; Moreno, M. T. *Inorg. Chem.* **2004**, *43*, 8185−8198.
(44) Shin, K.-S.; Son, K.-I.; Kim, J.-I.; Hong, C. S.; Suh, M.; Noh, D.-Y. *Dalton Trans.* **2009**, 1767−1775.
(45) Nihei, M.; Kurihara, M.; Mizutani, J.; Nishihara, H. *Chem. Lett.* **2001**, 852−853.
(46) Nihei, M.; Kurihara, M.; Mizutani, J.; Nishihara, H. *J. Am. Chem. Soc.* **2003**, *125*, 2964−2973.
(47) Bacsa, J.; Darkwa, J.; Maisela, L. L. *Acta Crystallogr., Sect. E* **2001**, *57*, m109−m110.
(48) Hunt, S. W.; Yang, L.; Wang, X.; Nesterov, V.; Richmond, M. G. *J. Inorg. Organomet. Polym.* **2010**, *20*, 457−467.
(49) Chandrasekaran, P.; Arumugam, K.; Jayarathne, U.; Pérez, L. M.; Mague, J. T.; Donahue, J. P. *Inorg. Chem.* **2009**, *48*, 2103−2113.
(50) Chandrasekaran, P.; Donahue, J. P. *Org. Synth.* **2009**, *86*, 333−343.
(51) Armarego, W. L. F.; Perrin, D. D. *Purification of Laboratory Chemicals*, 4th ed.; Butterworth-Heinemannn: Oxford, U.K., 2000.
(52) Pollock, C. J.; Tan, L. L.; Zhang, W.; Lancaster, K. M.; Lee, S. C.; DeBeer, S. *Inorg. Chem.* **2014**, *53*, 2591−2597.
(53) George, G. N. *EXAFSPAK*; Stanford Synchrotron Radiation Laboratory, Stanford Linear Accelerator Center, Stanford University: Stanford, CA, 2001.
(54) Bhattacharya, A. K.; Hortmann, A. G. *J. Org. Chem.* **1974**, *39*, 95−97.
(55) Levi, O. P.-T.; Becker, J. Y.; Ellern, A.; Khodorkovsky, V. *Tetrahedron Lett.* **2001**, *42*, 1571−1573.
(56) Arumugam, K.; Clark, D. S.; Mague, J. T.; Donahue, J. P. *Acta Crystallogr., Sect. C* **2011**, *67*, o446−o449.
(57) Xue, G.; Fang, Q.; Yu, W.-T.; Chen, X.; Lei, H. *J. Chem. Crystallogr.* **2008**, *38*, 65−69.
(58) Xue, G.; Fang, Q.; Yu, W. *Acta Crystallogr., Sect. C* **2003**, *59*, o653−o655.
(59) Simonsen, O.; Varma, K. S.; Clark, A.; Underhill, A. E. *Acta Crystallogr., Sect C* **1990**, *46*, 804−807.
(60) Ma, C.; Han, Y.; Li, D. *Polyhedron* **2004**, *23*, 1207−1216.
(61) Allan, G. M.; Howie, R. A.; Skakle, J. M. S.; Wardell, J. L.; Wardell, S. M. S. V. *J. Organomet. Chem.* **2001**, *627*, 189−200.
(62) Chohan, Z. H.; Howie, R. A.; Wardell, J. L. *J. Organomet. Chem.* **1999**, *577*, 140−149.

(63) Doidge-Harrison, S. M. S. V.; Irvine, J. T. S.; Khan, A.; Spencer, G. M.; Wardell, J. L.; Aupers, J. H. *J. Organomet. Chem.* **1996**, *516*, 199−205.
(64) Dessy, G.; Fares, V.; Bellitto, C.; Flamini, A. *Cryst. Struct. Commun.* **1982**, *11*, 1743−1745.
(65) Hursthouse, M. B.; Malik, K. M. A.; Underhill, A. Private Communication to CSD, 2003, Entry QAYMOT.
(66) (a) Kogut, E.; Tang, J. A.; Lough, A. J.; Widdifield, C. M.; Schurko, R. W.; Fekl, U. *Inorg. Chem.* **2006**, *45*, 8850−8852. (b) Tang, J. A.; Kogut, E.; Norton, D.; Lough, A. J.; McGarvey, B. R.; Fekl, U.; Schurko, R. W. *J. Phys. Chem. B* **2009**, *113*, 3298−3313.
(67) Gritsenko, V. V.; Ýyachenko, O. A.; Cassoux, P.; Kotov, A. I.; Laukhina, E. E.; Faulmann, C.; Yagubskii, E. B. *Russ. Chem. Bull.* **1993**, *42*, 1149−1151.
(68) Zhou, B.; Kobayashi, A.; Okano, Y.; Nakashima, T.; Aoyagi, S.; Nishibori, E.; Sakata, M.; Tokumoto, M.; Kobayashi, H. *Adv. Mater.* **2009**, *21*, 3596−3600.
(69) Okuma, K.; Munakata, K.; Tsubota, T.; Kanto, M.; Nagahora, N.; Shioji, K.; Yokomori, Y. *Tetrahedron* **2012**, *68*, 6211−6217.
(70) Suzuki, W.; Fujiwara, E.; Kobayashi, A.; Hasegawa, A.; Miyamoto, T.; Kobayashi, H. *Chem. Lett.* **2002**, 936−937.
(71) Arca, M.; Demartin, F.; Devillanova, F. A.; Garau, A.; Isaia, F.; Lelj, F.; Lippolis, V.; Pedraglio, S.; Verani, G. *J. Chem. Soc., Dalton Trans.* **1998**, 3731−3736.
(72) Lim, B. S.; Fomitchev, D. V.; Holm, R. H. *Inorg. Chem.* **2001**, *40*, 4257−4262.
(73) Arumugam, K.; Bollinger, J.; Fink, M.; Donahue, J. P. *Inorg. Chem.* **2007**, *46*, 3283−3288.
(74) Taylor, J. R. *An Introduction to Error Analysis*; University Science Books: Sausalito, CA, 1997; pp 73−77.
(75) Szilagyi, R. K.; Lim, B. S.; Glaser, T.; Holm, R. H.; Hedman, B.; Hodgson, K. O.; Solomon, E. I. *J. Am. Chem. Soc.* **2003**, *125*, 9158−9169.
(76) Samar, D.; Harvey, P. D. *J. Inorg. Organomet. Polym.* **2007**, *17*, 251−258.
(77) Lobana, T. S.; Sharma, R.; Bermejo, E.; Castineiras, A. *Inorg. Chem.* **2003**, *42*, 7728−7730.
(78) Pop, F.; Branzea, D. G.; Cauchy, T.; Avarvari, N. *C. R. Chim.* **2012**, *15*, 904−910.
(79) In ref 78, the structure of $[(Ph_3P)Pd(\mu\text{-}S_2C_2H_2)_2Pd(PPh_3)]$ is incorrectly described as residing on an inversion center. The molecule occurs on a 2-fold rotation axis.
(80) Cao, R.; Jiang, F.; Liu, H. *Acta Crystallogr., Sect. C* **1995**, *51*, 1280−1282.
(81) Nakanishi, I.; Tanaka, S.; Matsumoto, K.; Ooi, S. *Acta Crystallogr., Sect. C* **1994**, *50*, 58−61.
(82) Fenn, R. H.; Segrott, G. R. *J. Chem. Soc. A* **1970**, 3197−3201.
(83) Fenn, R. H.; Segrott, G. R. *J. Chem. Soc., Dalton Trans.* **1972**, 330−333.
(84) Estudiante-Negrete, F.; Redón, R.; Hernández-Ortega, S.; Toscano, R. A.; Morales-Morales, D. *Inorg. Chim. Acta* **2007**, *360*, 1651−1660.
(85) Ananikov, V. P.; Kabeshov, M. A.; Beletskaya, I. P.; Khrustalev, V. N.; Antipin, M. Y. *Organometallics* **2005**, *24*, 1275−1283.
(86) See http://periodictable.com/Elements/046/data.html (last accessed: May 19, 2014).
(87) Arumugam, K.; Shaw, M. C.; Mague, J. T.; Bill, E.; Sproules, S.; Donahue, J. P. *Inorg. Chem.* **2011**, *50*, 2995−3002.
(88) Glaser, T.; Hedman, B.; Hodgson, K. O.; Solomon, E. I. *Acc. Chem. Res.* **2000**, *33*, 859−868.
(89) Sarangi, R.; DeBeer George, S.; Rudd, D. J.; Szilagyi, R. K.; Ribas, X.; Rovira, C.; Almeida, M.; Hodgson, K. O.; Hedman, B.; Solomon, E. I. *J. Am. Chem. Soc.* **2007**, *129*, 2316−2326.
(90) DeBeer George, S.; Neese, F. *Inorg. Chem.* **2010**, *49*, 1849−1853.
(91) Ray, K.; DeBeer George, S.; Solomon, E. I.; Wieghardt, K.; Neese, F. *Chem.—Eur. J.* **2007**, *13*, 2783−2797.
(92) Jayarathne, U.; Chandrasekaran, P.; Greene, A. F.; Mague, J. T.; DeBeer, S.; Lancaster, K. M.; Sproules, S.; Donahue, J. P. *Inorg. Chem.* **2014**.
(93) Yan, Y.; Keating, C.; Chandrasekaran, P.; Jayarathne, U.; Mague, J. T.; DeBeer, S.; Lancaster, K. M.; Sproules, S.; Rubtsov, I. V.; Donahue, J. P. *Inorg. Chem.* **2013**, *52*, 6743−6751.
(94) Yan, Y.; Chandrasekaran, P.; Mague, J. T.; DeBeer, S.; Sproules, S.; Donahue, J. P. *Inorg. Chem.* **2012**, *51*, 346−361.
(95) Ward, M. D.; McCleverty, J. A. *Dalton Trans.* **2002**, 275−288.